Electronic Supplementary Information

Synthesis, DNA binding, docking and photocleavage studies of quinolinyl chalcones

P. J. Bindu,*[,a] K. M. Mahadevan,[a] T. R. Ravikumar Naik,[b] B.G. Harish[c]

Table of Contents:

Materials and equipment

All the chemicals used in the present study are of AR grade. Whenever analytical grade chemicals were not available, laboratory grade chemicals were purified and used. Calf thymus DNA (CT DNA) and supercoiled pUC19 DNA (cesium chloride purified) was obtained from Bangalore Genei (India). Agarose (low melt, 65°C, molecular biology grade for DNA gels), ethidium bromide, bromophenol blue, Tris(hydroxymethyl)aminomethane (Tris), sodium chloride, ethylene diamine tetraacetic acid disodium salt (EDTA-Na_2), sodium azide, were of molecular biology grade, obtained from Himedia (India).

Melting points were recorded on an open capillary tube with a Buchi melting point apparatus and are uncorrected. Elemental analyses were carried out using Perkin-Elmer 240C CHN-analyzer. IR spectra were recorded on a FT-IR infrared spectrophotometer. ^{1}H- NMR spectra were obtained using a 300 MHz and 400 MHz on a Bruker spectrometer (chemical shifts in δ ppm). Mass spectra were recorded using a micro spray Q-TOF MS ES Mass spectrometer.

4.1 General procedure for the preparation 2-chloro-3-quinolinyl-3-phenylpropen-2-ones:

To a stirred solution of acetophenone (0.6 g, 5.2 mmol) and (1.0 g, 5.2 mmol) 2-chloro-3-formylquinoline dissolved in 10 mL 95 % ethanol containing 2 mL 2.5 M NaOH (aq). The resulting solution was stirred at room temperature and within five minutes the mixture was precipitated. After one hour, the reaction mixture was kept over night at 0-5 °C and then it was poured into cold water, filtered, and the solid rinsed with water and cold ethanol. The crude product thus obtained was recrystallized from MeOH to obtain desired product (Scheme 1, Table 1).

(E)-3-(2-chloroquinolin-3-yl)-1-phenylprop-2-en-1-one (3a)[29]: M.p: 180-182 °C; IR (Neat): 1680 (C=O), 1559 (C=C) cm^{-1}; ^{1}H NMR (400 MHz, $CDCl_3$): δ = 7.45-7.56 (d, 2H, *J* = 8.0, Ar-H), 7.61-7.64 (t, 1H, *J* = 8.0), 7.76-7.77, (d, 1H, *J* = 8.0), 7.78-7.79 (d, 1H, *J* = 8.0, Ar-H), 7.86-7.90 (d, 1H, H_α, *J* = 16.0), 7.96-7.98 (d, 1H, *J* = 8.0), 8.07-8.17 (d, 1H, *J* = 8.0), 8.19-8.23 (d, 1H, H_β, *J* = 16.0), 8.53 (s, 1H) ppm; MS (m/z) 316 (M+23), Calcd (293), Found (316); Anal. Calcd (%) for $C_{18}H_{12}ClNO$: C; 73.60, H; 4.12, N; 4.77. Found: C; 73.58, H; 4.10, N; 4.75.

(E)-3-(2-chloroquinolin-3-yl)-1-(4-methylphenyl)prop-2-en-1-one (3b): M.p: 151-153 °C; IR (Neat): 1662 (C=O), 1487 (C=C) cm^{-1}; cm^{-1}; ^1H NMR (400 MHz, $CDCl_3$): δ = 2.43 (s, 3H, CH_3), 7.30-7.32 (d, 2H, *J* = 8.0, Ar-H), 7.35 (d, 1H, *J* = 8.0, Ar-H), 7.57-7.58 (d, 1H, *J* = 8.0), 7.59-7.64 (d, 1H, H_α, *J* = 16.0), 7.73-7.77 (t, 1H, *J* = 8.0), 7.85-7.88 (t, 1H, *J* = 8.0), 7.95-7.97 (d, 1H, *J* = 8.0), 7.99-8.01 (d, 1H, *J* = 8.0), 8.14-8.18 (d, 1H, H_β, *J* = 16.0), 8.50 (s, 1H) ppm; ^{13}C NMR (400 MHz, $CDCl_3$): δ = 42.3 (CH_3), 126.2, 126.9, 127.2, 127.9, 128.5, 128.6(Cq), 131.5, 133.2, 134.8(Cq), 137.4(Cq), 139.2(Cq), 146.2(Cq), 147.7(Cq), 150.3(Cq), 150.5(Cq), 189.7 ppm; MS (m/z) 330 (M+23), Calcd (307), Found (330); Anal. Calcd (%) for $C_{19}H_{14}ClNO$: C; 74.15, H; 4.58, N; 4.55. Found: C; 74.13, H; 4.56, N; 4.53.

(E)-3-(2-chloroquinolin-3-yl)-1-(4-methoxyphenyl)prop-2-en-1-one (3c): M.p: 226-228 °C; IR (Neat): 1656 (C=O), 1570, 1511 (C=C) cm^{-1}; ^1H NMR (400 MHz, $CDCl_3$): δ = 3.90 (s, 3H, OCH_3), 6.99-7.01 (d, 2H, *J* = 8.0, Ar-H), 7.60-7.64 (2d, 2H, *J* = 8.0, Ar-H), 7.75-7.79 (t, 1H, H_α, *J* = 16.0), 7.87-7.89 (d, 1H, *J* = 8.0), 8.01-8.03 (d, 1H, *J* = 8.0), 8.06-8.08 (d, 1H, *J* = 8.0), 8.15-8.19 (d, 1H, H_β, *J* = 16.0), 8.50 (s, 1H), ppm; ^{13}C NMR (400 MHz, $CDCl_3$): δ = 52.32 (OCH_3), 110.7, 123.0, 123.7, 124.4, 124.7, 125.0, 125.2(Cq), 127.2(Cq), 127.8(Cq), 128.2(Cq), 132.8, 135.2(Cq), 144.5(Cq), 147.1(Cq), 160.5(Ar-O), 184.7 (C=O) ppm; MS (m/z) 346 (M+23), Calcd (323), Found (346); Anal. Calcd (%) for $C_{19}H_{14}ClNO_2$: C; 70.48, H; 4.36, N; 4.33. Found: C; 70.46, H; 4.34, N; 4.31.

(E)-3-(2-chloroquinolin-3-yl)-1-(4-hydroxyphenyl)prop-2-en-1-one (3d): M.p: 178-181°C; IR (Neat): 1653 (C=O), 1459 (C=C) cm^{-1}; ^1H NMR (400 MHz, $CDCl_3$): δ = 6.92-6.94 (d, 2H, *J* = 8.0, Ar-H), 6.96-7.00 (d, 1H, H_α, *J* = 16.0), 7.05-7.07 (d, 1H, *J* = 8.0, Ar-H), 7.49-7.51 (d, 1H, *J* = 8.0), 7.51-7.53 (d, 1H, *J* = 8.0), 7.71-7.88 (t, 1H, *J* = 8.0), 7.92-7.96 (d, 1H, H_α, *J* = 16.0), 8.00-8.17 (t, 1H, *J* = 8.0), 8.31-8.35 (d, 1H, H_β, *J* = 16.0), 8.79 (s, 1H), 10.45 (OH, 1H) ppm; ^{13}C NMR (400 MHz, $CDCl_3$): δ = 113.8, 126.1, 126.8, 127.5, 127.8, 128.1, 128.3(Cq), 130.3(Cq), 130.9(Cq), 131.3(Cq), 135.9, 138.3(Cq), 147.6(Cq), 150.2(Cq), 163.6(Ar-O), 187.8 (C=O) ppm; MS (m/z) 332 (M+23), Calcd (309), Found (332); Anal. Calcd (%) for $C_{18}H_{12}ClNO_2$: C; 69.80, H; 3.90, N; 4.52. Found: C; 69.78, H; 3.88, N; 4.53.

(E)-3-(2-chloroquinolin-3-yl)-1-(4-chlorophenyl)prop-2-en-1-one (3e): M.p: 170-173 °C; IR (Neat): 1604 (C=O), 1459 (C=C) cm^{-1}; ^1H NMR (400 MHz, $CDCl_3$): δ = 7.24-7.28 (d, 1H, *J* = 8.0), 7.40-7.42 (d, 2H, *J* = 8.0), 7.59-7.63 (t, 1H, *J* = 8.0), 7.78-7.82 (d, 1H, H_α, *J* = 16.0), 7.94-7.97 (d, 2H, *J* = 8.0, Ar-H), 8.04-8.06 (d, 1H, *J* = 8.0), 8.17-8.19 (d, 2H, *J* = 8.0, Ar-H), 8.32-8.36 (d, 1H, H_β, *J* = 16.0), 8.62 (s, 1H) ppm; ^{13}C NMR (400 MHz, $CDCl_3$): δ = 119.6, 119.7, 127.0, 127.1, 128.0, 128.9, 128.9, 129.9(Cq), 130.1(Cq), 134.4(Cq), 136.2(Cq), 137.0, 139.8(Cq), 146.3(Cq), 150.3(Cq-Cl), 196.5 (C=O) ppm; MS (m/z) 350 (M+23), Calcd (327), Found (350); Anal. Calcd (%) for $C_{18}H_{11}Cl_2NO$: C; 65.87, H; 3.38, N; 4.27. Found: C; 65.85, H; 3.36, N; 4.25.

(E)-3-(2-chloroquinolin-3-yl)-1-(4-bromophenyl)prop-2-en-1-one (3f): M.p: 187-189 °C; IR (Neat): 1607 (C=O), 1511 (C=C) cm^{-1}; ^1H NMR (400 MHz, $CDCl_3$): δ = 7.37-7.39 (d, 1H, *J* = 8.0, Ar-H), 7.57-7.60 (t, 1H, *J* = 8.0), 7.74-7.76 (d, 1H, *J* = 8.0), 7.79-7.81 (d, 2H, *J* = 8.0, Ar-H), 7.82-7.86 (d, 1H, H_α, *J* = 16.0), 7.98-7.80 (d, 1H, *J* = 8.0), 8.14-8.16 (d, 1H, *J* = 8.0), 8.29-8.33 (d, 1H, H_β, *J* = 16.0), 8.51 (s, 1H) ppm; MS (m/z) 395 (M+23), Calcd (372), Found (395); Anal. Calcd (%) for $C_{18}H_{11}BrClNO$: C; 58.02, H; 2.98, N; 3.76. Found: C; 58.00, H; 2.96, N; 3.74.

(E)-3-(2-chloroquinolin-3-yl)-1-(4-nitrophenyl)prop-2-en-1-one (3g): M.p: 165-167 °C; IR (Neat): 1658 (C=O), 1523 (C=C) cm^{-1}; ^1H NMR (400 MHz, $CDCl_3$): δ = 7.25-7.28 (t, 1H, *J* = 8.0), 7.35-7.37 (d, 1H, *J* = 8.0), 7.58-7.61 (t, 1H, *J* = 8.0), 7.73-7.75 (d, 1H, *J* = 8.0, Ar-H), 7.81-7.83 (d, 1H, *J* = 8.0, Ar-H), 7.85-7.89 (d, 1H, H_α, *J* = 16.0), 8.03-8.05 (d, 1H, *J* = 8.0), 8.19-8.23 (d, 1H, H_β, *J* = 16.0), 8.60 (s, 1H) ppm; MS (m/z) 361 (M+23), Calcd (338), Found (361); Anal. Calcd (%) for $C_{18}H_{11}ClN_2O_3$: C; 63.82, H; 3.27, N; 8.27. Found: C; 63.80, H; 3.25, N; 8.25.

(E)-3-(2-chloroquinolin-3-yl)-1-(4-(methylamino)phenyl)prop-2-en-1-one (3h): M.p: 165-167 °C; IR (Neat): 1647 (C=O), 1590, 1552 (C=C) cm^{-1}; ^1H NMR (400 MHz, $CDCl_3$): δ = 4.875 (S, $NHCH_3$), 7.33-7.35 (d, 1H, *J* = 8.0), 7.38-7.40 (d, 1H, *J* = 8.0), 7.41-7.42 (d, 2H, *J* = 8.0, Ar-H), 7.58-7.63 (t, 1H, *J* = 8.0), 7.75-7.79 (t, 1H, *J* = 8.0), 7.95 (d, 1H, H_α, *J* = 16.0), 8.03-8.05 (d, 1H, *J* = 8.0, Ar-H), 8.06-8.10 (d, 1H, H_β, *J* = 16.0), 8.61 (s, 1H) ppm; ^{13}C NMR (400 MHz, $CDCl_3$): ^{13}C NMR (400 MHz, $CDCl_3$): δ = 33.1 (CH_3), 117, 120.0, 123.4, 124.5, 127.0, 127.4, 127.6, 128.2(Cq),

128.3, 130.0(Cq), 131.2(Cq), 136.8(Cq), 138.1(Cq), 147.1(Cq), 149.9(Cq), 186.1 ppm.

UV-visible absorbance spectral studies

All the experiments involving interaction of the 2-chloro-3-quinolinyl-3-phenylpropen-2-ones with CT-DNA were carried out in doubly distilled H_2O buffer containing 5 mM Tris and 50 mM NaCl and adjusted to pH 7.2 with hydrochloric acid. A solution of CT-DNA gave a ratio of UV absorbance at 260 and 280 nm of about 1.8-1.9, indicating that the CT-DNA was sufficiently free of protein. The CT-DNA concentration per nucleotide was determined spectrophotometrically by employing an extinction coefficient of 6600 M^{-1} cm^{-1} at 260 nm. The 2-chloro-3-quinolinyl-3-phenylpropen-2-ones were dissolved in a solvent mixture of 10% DMSO and 90% Tris-HCl buffer (5 mM Tris–HCl, 50 mM NaCl, pH 7.2) at concentration 10.0 x 10^{-6} M. An absorption titration experiment was performed by maintaining the 10 μM compounds and varying the concentration of nucleic acid. While measuring the absorption spectra, an equal amount of CT-DNA was added to both the compound solution and the reference solution to eliminate the absorbance of CT-DNA itself. The absorption data were analyzed for an evaluation of the intrinsic binding constant K_b. The observed values for the2-chloro-3-quinolinyl-3-phenylpropen-2-ones were then calculated by the equation 1 to obtain the intrinsic binding constant K_b.

$$[DNA]/(\varepsilon_a-\varepsilon_f) = [DNA]/(\varepsilon_b-\varepsilon_f) + 1/K_b(\varepsilon_a-\varepsilon_f) \text{----------(equation 1)}$$

Where ε_a, ε_f and ε_b are the apparent, free and bound metal complex extinction coefficients, respectively. A plot of [DNA]/ ($\varepsilon_b-\varepsilon_f$) *versus* [DNA] gave a slope of $1/(\varepsilon_b-\varepsilon_f)$ and a y intercept equal to $1/K_b(\varepsilon_b-\varepsilon_f)$, where K_b is the ratio of the slope to the y intercept.

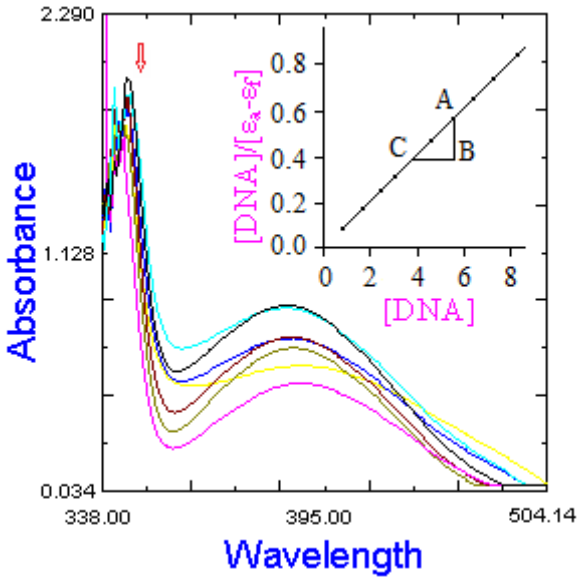

Fig. 1(a). UV absorption spectra of **3a** upon addition of calf thymus (ds) DNA. **3a**; control [DNA] = 0.5 μM [---], [**3a**] + [DNA] =10 μM; 20 μM; 30 μM; 40 μM DNA respectively. Arrow shows the absorbance changing upon the increase of DNA concentration. The inner plot of [DNA]/(ε_a-ε_f) *vs* [DNA] for the titration of DNA with **3a**.

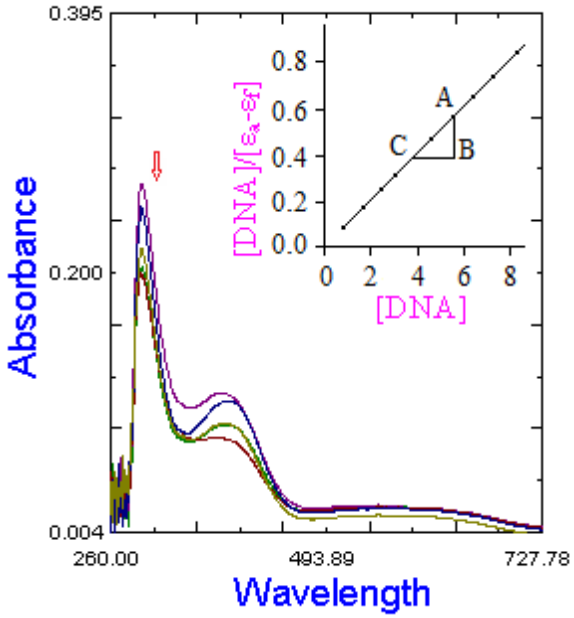

Fig. 1(b). UV absorption spectra of **3b** upon addition of calf thymus (ds) DNA. **3b**; control [DNA] = 0.5 μM [---], [**3b**] + [DNA] =10 μM [---]; 20 μM [---]; 30 μM [---] DNA respectively. Arrow shows the absorbance changing upon the increase of DNA concentration.

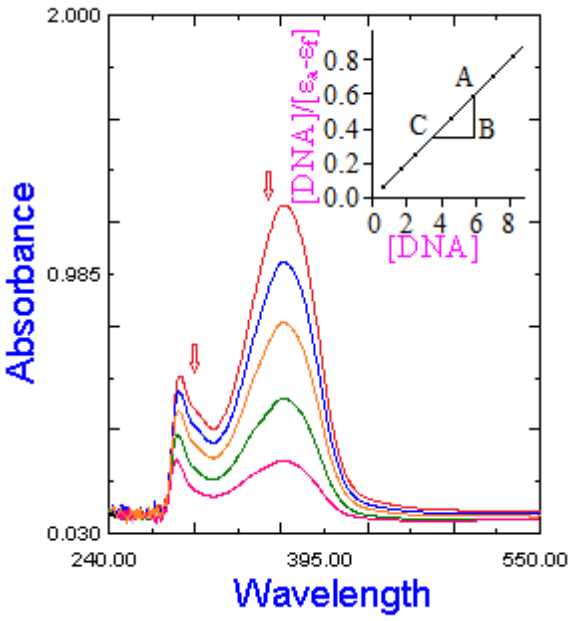

Fig. 1(c). UV absorption spectra of **3c** upon addition of calf thymus (ds) DNA. **3c**; control [DNA] = 0.5 μM [---], [**3c**] + [DNA] =10 μM [---]; 20 μM [---]; 30 μM [---]; 40 μM [---] DNA respectively. Arrow shows the absorbance changing upon the increase of DNA concentration. The inner plot of [DNA]/(ε_a-ε_f) *vs* [DNA] for the titration of DNA with **3c**.

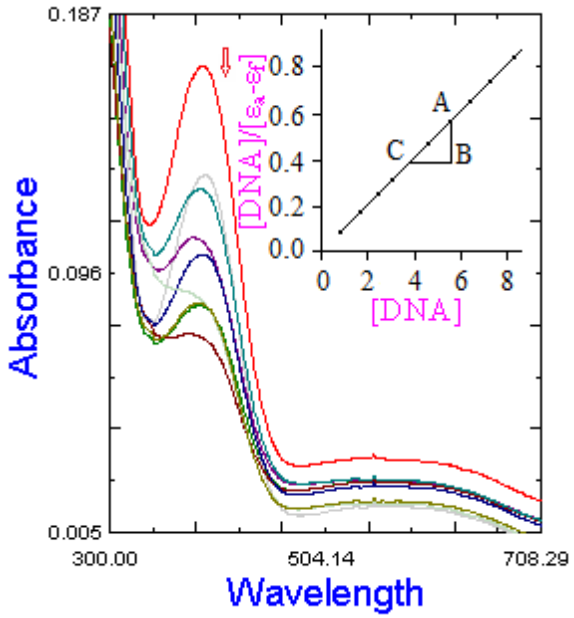

Fig. 1(d). UV absorption spectra of **3d** upon addition of calf thymus (ds) DNA. **3d**; control [DNA] = 0.5 μM [---], [**3d**] + [DNA] =10 μM [---]; 20 μM [---]; 30 μM [---]; 40 μM [---]; 50 μM [---] DNA respectively. Arrow shows the absorbance changing upon the increase of DNA concentration. The inner plot of [DNA]/(ε_a-ε_f) *vs* [DNA] for the titration of DNA with **3d**.

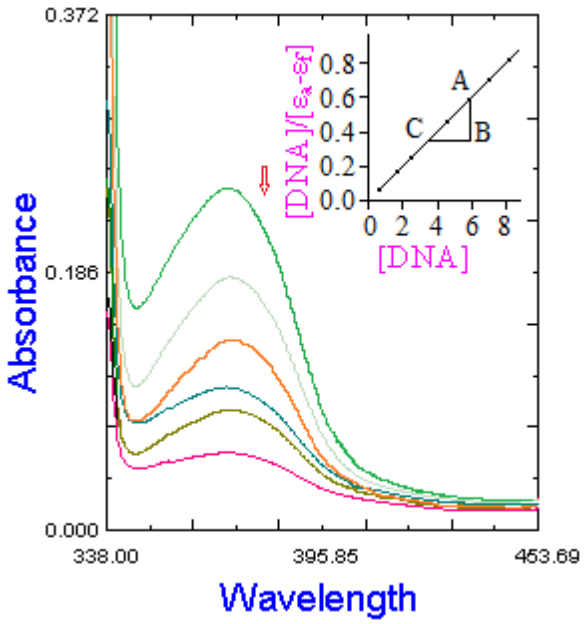

Fig. 1(e). UV absorption spectra of **3e** upon addition of calf thymus (ds) DNA. **3e**; control [DNA] = 0.5 μM [---], [**3e**] + [DNA] =10 μM [---]; 20 μM [---]; 30 μM [---]; 40 μM [---]; 50 μM [---] DNA respectively. Arrow shows the absorbance changing upon the increase of DNA concentration. The inner plot of [DNA]/(ε_a-ε_f) *vs* [DNA] for the titration of DNA with **3e**.

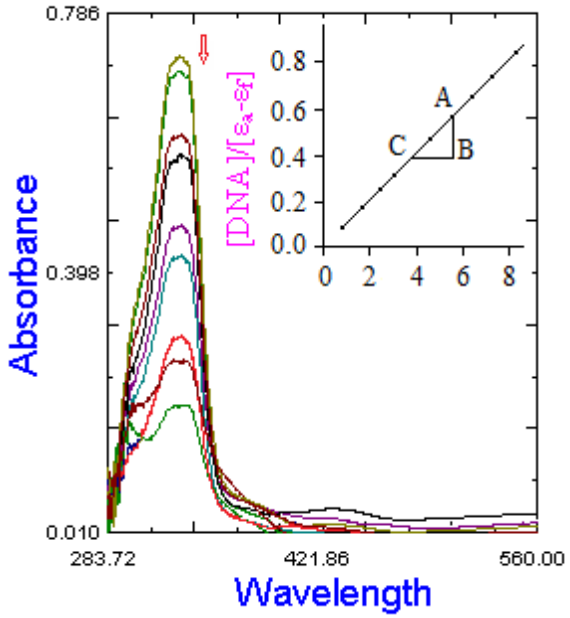

Fig. 1(g). UV absorption spectra of **3g** upon addition of calf thymus (ds) DNA. **3g**; control [DNA] = 0.5 μM [---], [**3g**] + [DNA] =10 μM [---]; 20 μM [---]; 30 μM [---]; 40 μM [---]; 50 μM [---]; 60 μM [---]; 70 μM [---]; 80 μM [---] DNA respectively. Arrow shows the absorbance changing upon the increase of DNA concentration. The inner plot of [DNA]/(ε_a-ε_f) *vs* [DNA] for the titration of DNA with **3g**.

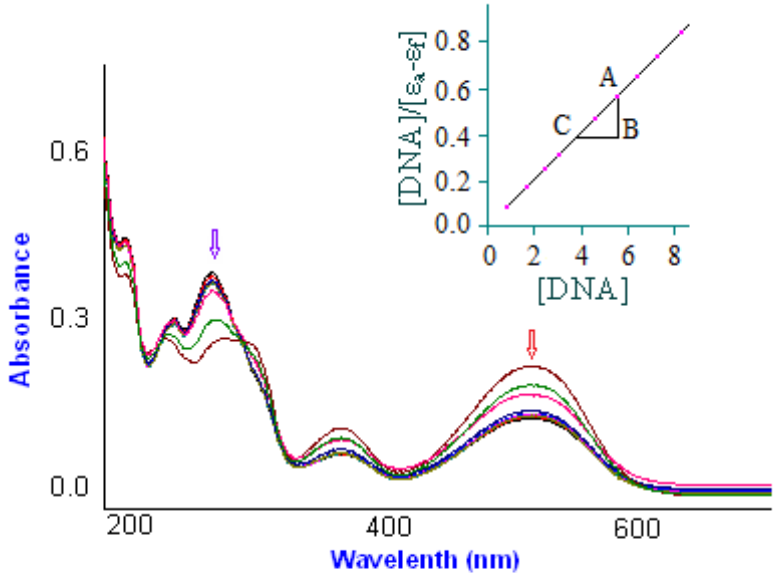

Fig. 1(h). UV absorption spectra of **3h** upon addition of calf thymus (ds) DNA. **3h**; control [DNA] = 0.5 µM [---], [**3h**] + [DNA] =10 µM [---]; 20 µM [---]; 30 µM [---]; 40 µM [---]; 50 µM [---] DNA respectively. Arrow shows the absorbance changing upon the increase of DNA concentration. The inner plot of [DNA]/(ε_a-ε_f) *vs* [DNA] for the titration of DNA with **3h**.

Fluorescence spectra

Fluorescence spectra were recorded on a Varian Cary Eclipse Fluorescence Spectrophotometer. Spectrophotometric measurements were performed in thermostated quartz sample cells of 10 mm pathlength at 20 °C. The CT-DNA concentration per nucleotide was determined spectrophotometrically by employing an extinction coefficient of 6600 M^{-1} cm^{-1} at 260 nm. The 2-chloro-3-quinolinyl-3-phenylpropen-2-ones were dissolved in a solvent mixture of 10% DMSO and 90% Tris-HCl buffer (5 mM Tris–HCl, 50 mM NaCl, pH 7.2) at concentration 10.0 x 10^{-6} M Figure 3. The prepared solutions were placed into quartz cells and titrated with the titrant solutions in intervals of 0.5-2 equivalent, and absorption spectra were recorded. All spectrophotometric titrations were performed at least 2-3 times to ensure the reproducibility. In addition the quenching constants K of QC (3a-g) were calculated according to the classical Stern-Volmer equation.[26]

$$I_0/I = 1 + Kr \text{---------- (equation 2)}$$

Where I_0 and I are the fluorescence intensities in the absence and presence of the QC and r is the ratio [QC]/[DNA]. The fluorescence quenching curves of

complexes are shown in Figure 3. The quenching plots illustrate that the binding of DNA by the complexes is in good agreement with the linear Stern-Volmer equation. In the linear fit plot of I_0/I *versus* [QC], the K values calculated, K= 3.8, 3.5, 4.2, 4.0, 3.3, 3.3, and 3.5 respectively. [24]

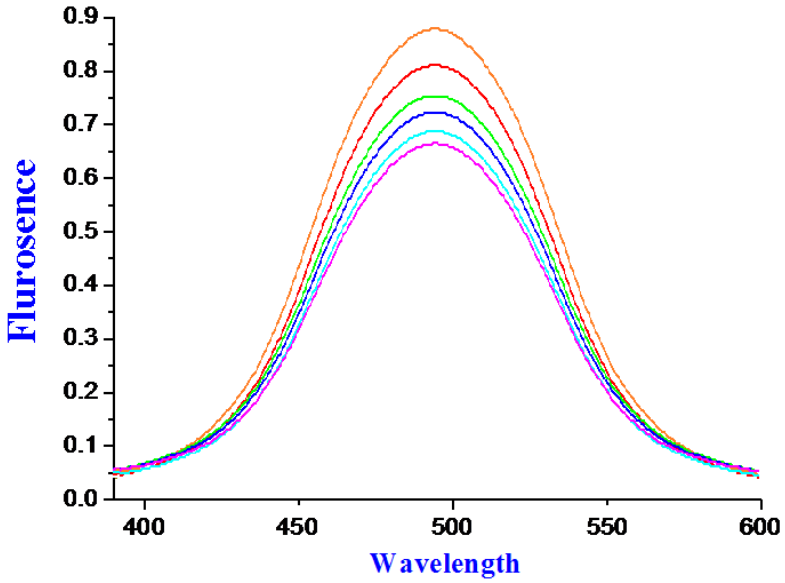

Fig. 2(a). The emission spectra of QC (3c) in the presence and absence of CT-DNA.

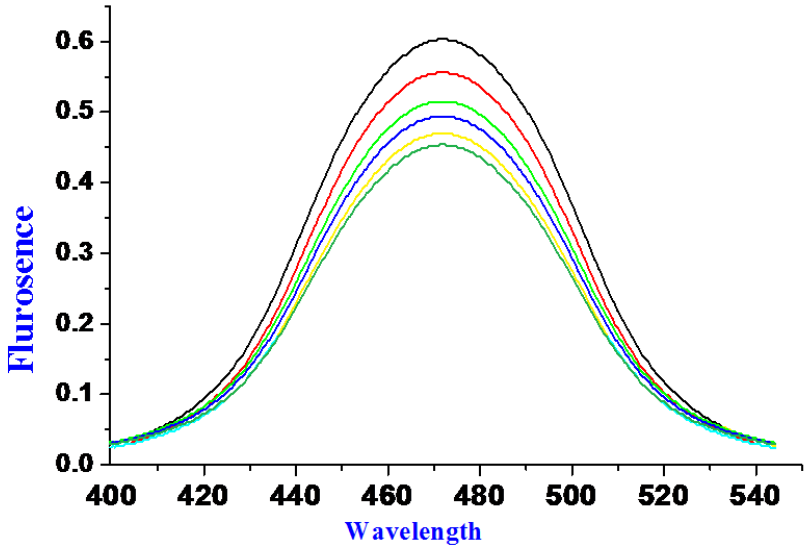

Fig. 2(b). The emission spectra of QC (3d) in the presence and absence of CT-DNA.

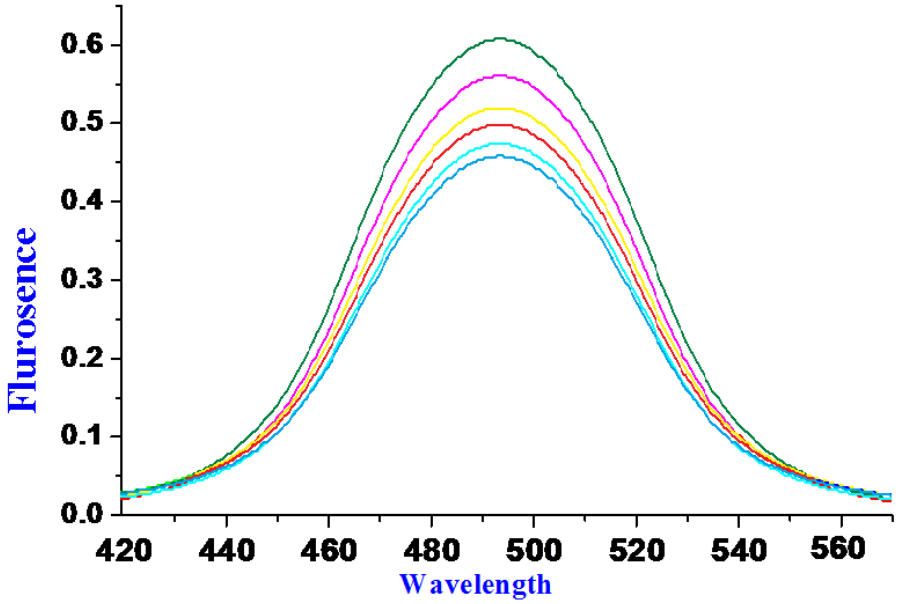

Fig. 2(c). The emission spectra of QC (3e) in the presence and absence of CT-DNA.

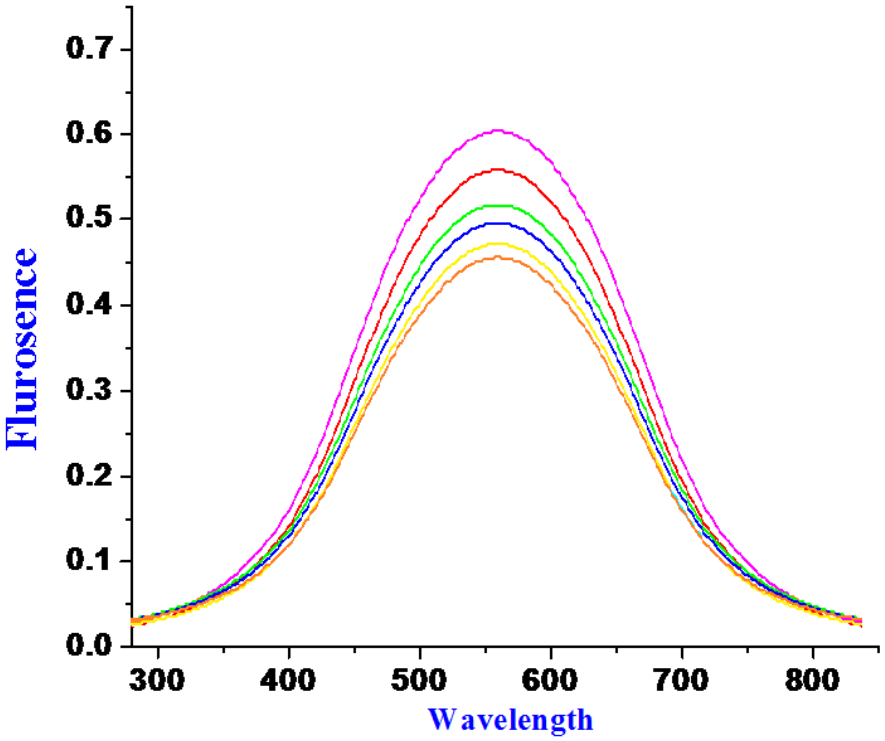

Fig. 2(d). The emission spectra of QC (3f) in the presence and absence of CT-DNA.

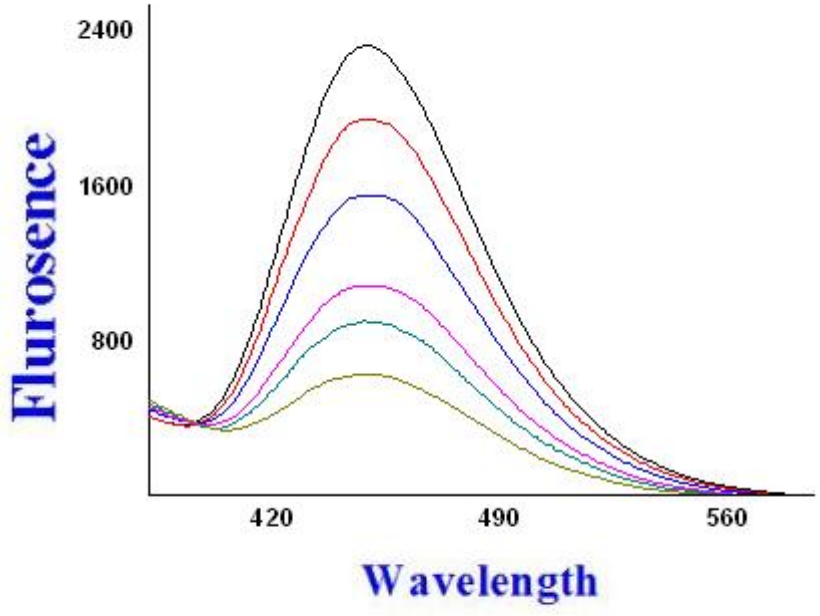

Fig. 2(e). The emission spectra of QC (3h) in the presence and absence of CT-DNA.

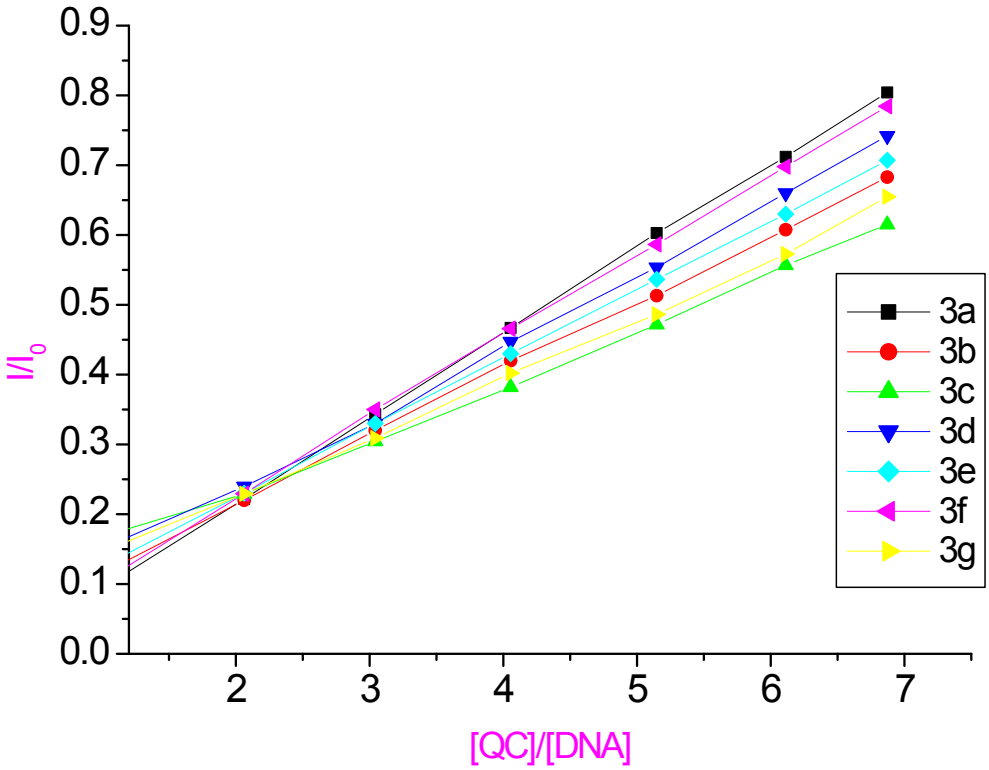

Fig. 3. The fluorescence quenching curves of QC (3a-g) in the presence and absence of CT-DNA.

Viscometric titration

Viscosity measurements were carried out using a semimicro dilution capillary viscometer at room temperature. Aliquots of the solution of the ligand in Tris-HCl buffer were added to the ct DNA solution (1 mM base pair in the Tris-HCl buffer). Flow times were measured after a thermal equilibration period of 5 min. Each flow time was measured three times and an average flow time value was calculated. As a reference ethidium bromide was employed under identical conditions. The relative viscosity was presented as $(\eta/\eta_0)^{1/3}$ Figure 4. The value η is the viscosity of the solution in the presence of a compound, calculated from the time for the sample (t_L) to flow through the viscometer subtracted by the time measured for the buffer (t_0) only (equation 3).

$$\eta = (t_L - t_0) / t_0 \quad \text{(Equation 3)}$$

η_0 is the viscosity of the ct DNA solution alone according to equation 4.

$$\eta_0 = (t - t_0) / t_0 \quad \text{(Equation 4)}$$

The relative viscosity $(\eta/\eta_0)^{1/3}$ was plotted as a function of ligand-to-DNA ratio,
r = Concentration of ligand/ Concentration of DNA

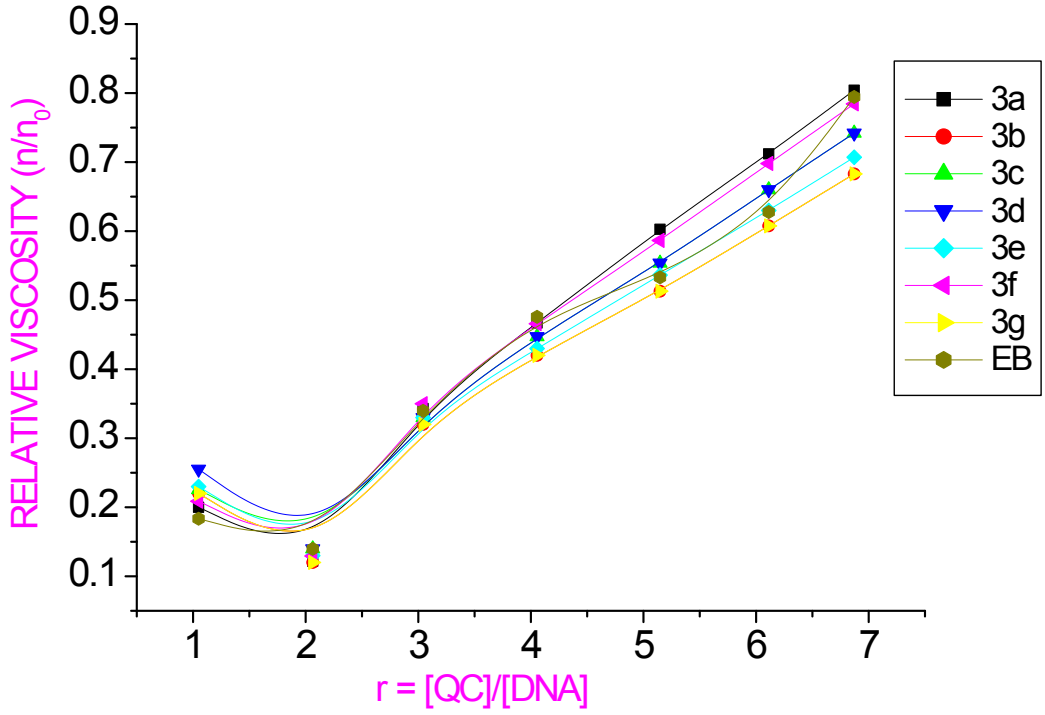

Fig. 4. Relative specific viscosity of ct DNA in the presence of **2** (circles) and ethidium bromide (triangles) as a function of the ligand-to-DNA ratio, *c*DNA = 1 mM bp in phosphate buffer.

Molecular docking

The 2-chloro-3-quinolinyl-3-phenylpropen-2-ones were designed and the structures were analyzed by using Chem-Draw Ultra 6.0 and it was subjected for geometrical optimization using MM2 and energy minimized by steepest gradient method in Chem3D ultra 6.0. The final selected conformation of 2-chloro-3-quinolinyl-3-phenylpropen-2-ones was tested for Lipinski's rule, drug toxicity and other properties through pre ADMET server. The small-molecule topology generator prodrug server automatically generates the coordinates for all the 2-chloro-3-quinolinyl-3-phenylpropen-2-ones. Automated docking was used to determine the orientation of inhibitors bind to the ds-DNA. A genetic algorithm method, implemented in the program Auto-Dock 3.0, was employed. The crystal structure of the B-DNA dodecamer, $d(CGCGAATTCGCG)_2$ (NBD code GDLB05) was obtained from the protein data bank. The coordinates for the heteroatom including water and other small molecules were removed. This structure was later added with polar hydrogens and kollmann charges to remove nonintergral chargers. For docking calculations, Gasteigere Marsili partial charges were assigned to the 2-chloro-3-quinolinyl-3-phenylpropen-2-ones and nonpolar hydrogen atoms were merged. All torsions were allowed to rotate during docking. Lennard- Jones parameters 12-10 and 12-6, supplied with the program, were used for modelling H-bonds and van der Waals interactions, respectively. The distance-dependent dielectric permittivity of Mehler and Solmajer was used to calculate the electrostatic grid maps. Random starting points, random orientation, and torsions were used for all ligands. The translation, quaternion, and torsion steps were taken from default values in Auto-Dock. The Lamarckian genetic algorithm and the pseudo-Solis and Wets methods were applied for minimization, using default parameters. The number of docking runs was 50, the population in the genetic algorithm was 250, the number of energy evaluations was 100,000, and the maximum number of iterations 10,000.

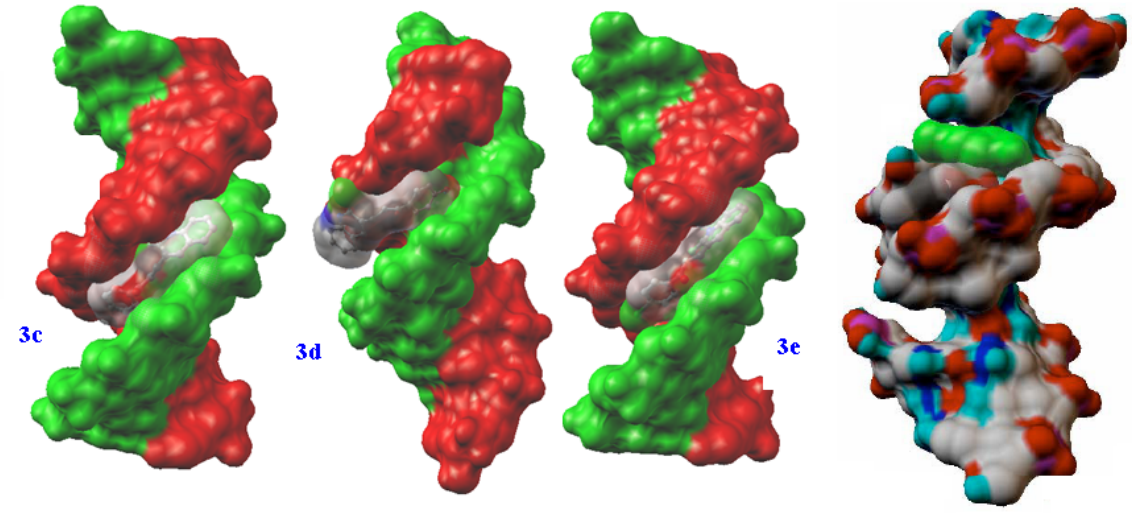

Fig-5

Fig. 5 View of the energy minimized docked poses of QC **3c, 3d, 3e** and **3h** with DNA d(CGCGAATTCGCG)$_2$ (PDB ID: 1BNA).

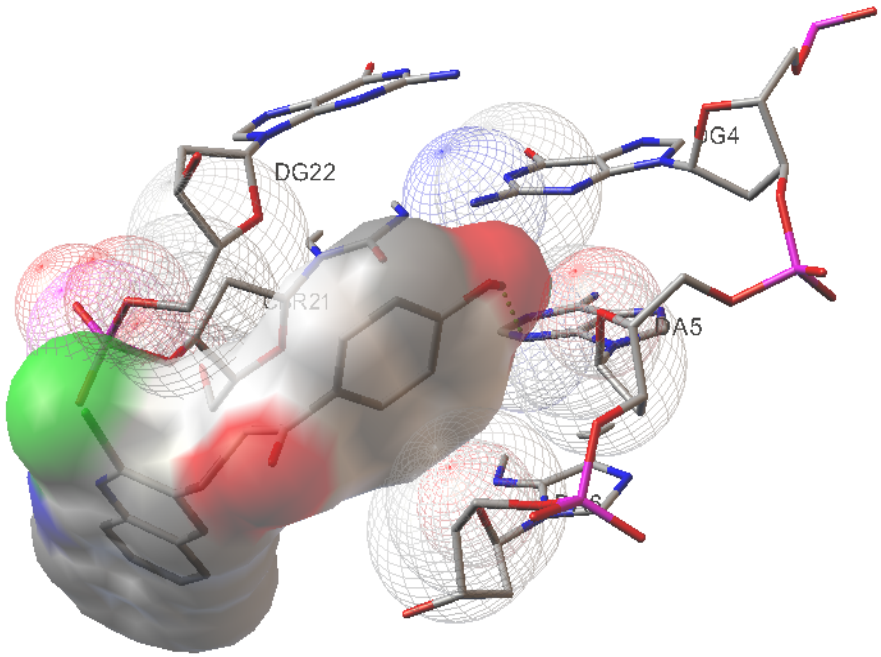

Fig. 6 (a) A molecular docked model of QC **3d** showing chemically significant hydrogen-bonding interactions with DNA d (CGCGAATTCGCG)$_2$ (PDB ID: 1BNA). **DNA**

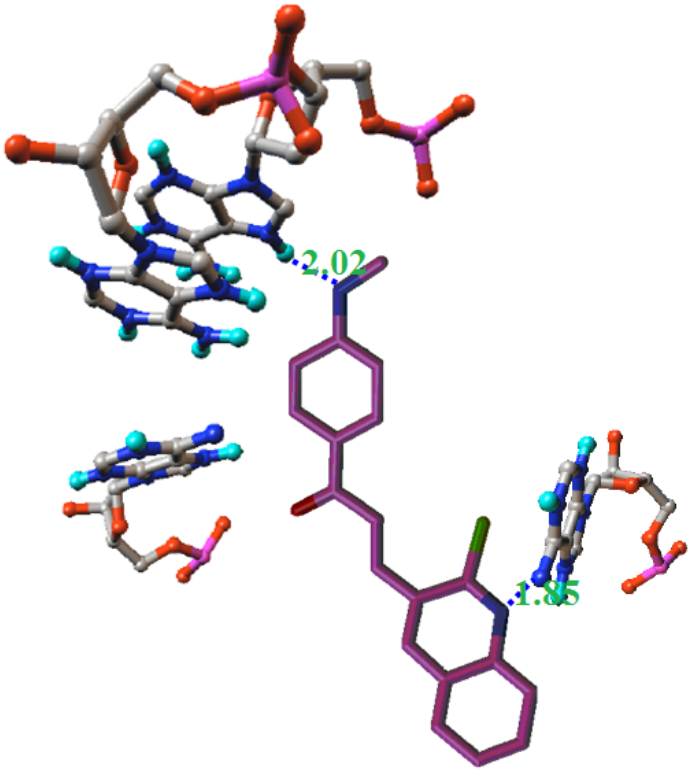

Fig. 6(b) A molecular docked model of QC **3h** showing chemically significant hydrogen-bonding interactions with DNA d $(CGCGAATTCGCG)_2$ (PDB ID: 1BNA).
DNA

Photocleavage by Gel Electrophoresis

For the gel electrophoresis experiments, supercoiled pUC19DNA (0.5µg) in Tris–HCl buffer (50mM) with 50mM NaCl (pH 7.2) was treated with 2-chloro-3-quinolinyl-3-phenylpropen-2-ones (40 and 80µM) and the solution was irradiated for 2h, in 1:9 DMSO: trisbuffer (20 µM, pH- 7.2) at 365 nm (10 W). After irradiation, the solution was incubated at 37 °C for 1 h. A loading buffer containing 25% bromophenol blue, 0.25% xylene cyanol and 30% glycerol. Electrophoresis was carried out for 3 h at 50V on a 0.8% agarose gel in Tris–boracic–EDTA buffer. The gel was stained with 1.0µg/ml ethidium bromide. Bands were visualized using UV light and photographed. The cleavage efficiency was measured by determining the ability of the 2-chloro-3-quinolinyl-3-phenylpropen-2-ones to convert the supercoiled DNA (SC) to nicked circular form (NC) and linear form (LC).

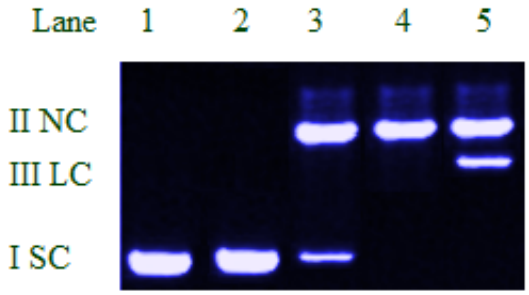

Fig. 7. Light-induced DNA cleavage by 2-chloro-3-quinolinyl-3-phenylpropen-2-ones at different concentration. The 2-chloro-3-quinolinyl-3-phenylpropen-2-ones were irradiated with UV light at 365 nm. Lane; 1: control DNA (without compound), Lane; 2: 20μM (**3d**), Lane; 3: 40μM (**3d**), Lane; 4: 60μM (**3d**), Lane; 5: 80μM (**3d**).

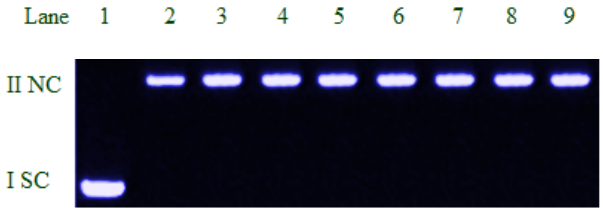

Fig. 8. Light-induced cleavage of DNA by quinolinyl chalcones at 365 nm. Lane; 1: control DNA (without compound), Lane; 2: 60μM (**3a**), Lane; 3: 60μM (**3b**), Lane; 4: 60μM (**3c**), Lane; 5: 60μM (**3d**), Lane; 6: 60μM (**3e**), Lane; 7: 60μM (**3f**), Lane; 8: 60μM (**3g**), 9; 60μM (**3h**).

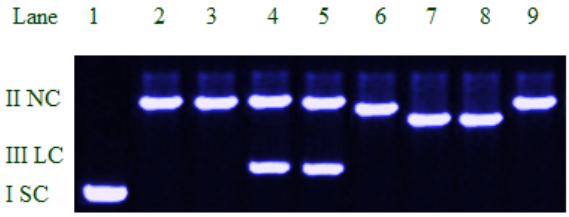

Fig. 9. Light-induced cleavage of DNA by quinolinyl chalcones at 365 nm. Supercoiled DNA runs at position I (SC), linear DNA at position III (LC) and nicked DNA at position II (NC). Lane; 1: control DNA (without compound), Lane; 2: 80μM (**3a**), Lane; 3: 80μM (**3b**), Lane; 4: 80μM (**3c**), Lane; 5: 80μM (**3d**), Lane; 6: 80μM (**3e**), Lane; 7: 80μM (**3f**), Lane; 8: 80μM (**3g**), 9; 60μM (**3h**).

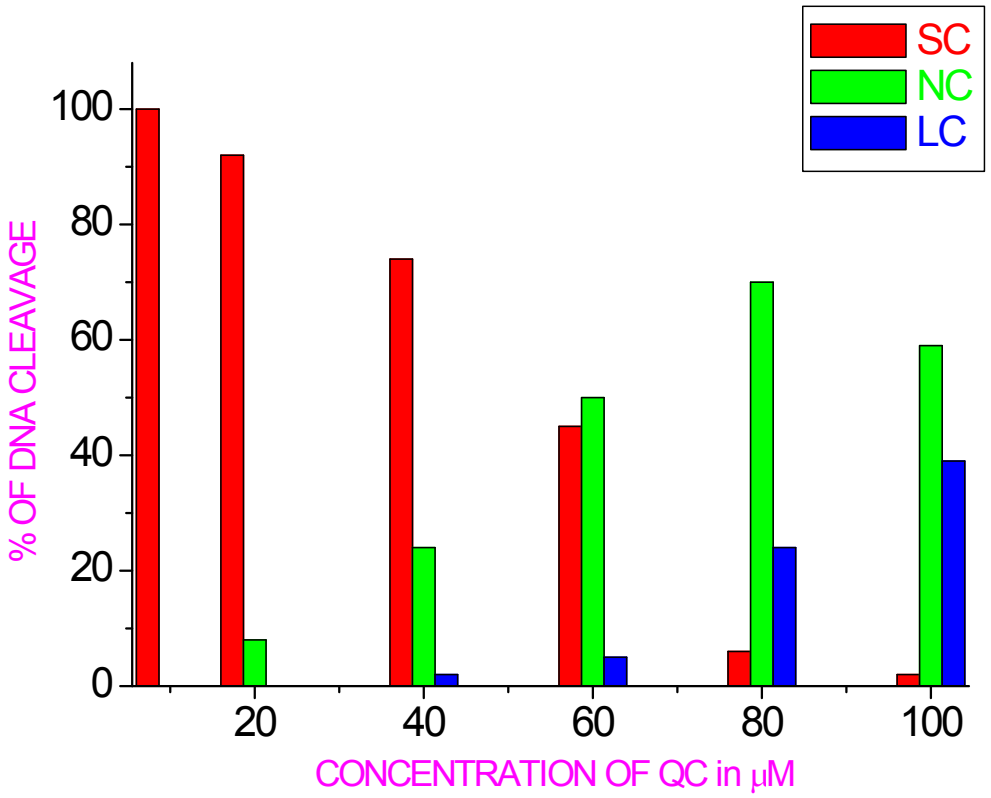

Fig. 10. Plot representation the percentage of pUC 19 DNA cleavage with different concentrations of2-chloro-3-quinolinyl-3-phenylpropen-2-ones (20-100 μM) at 37 °C.

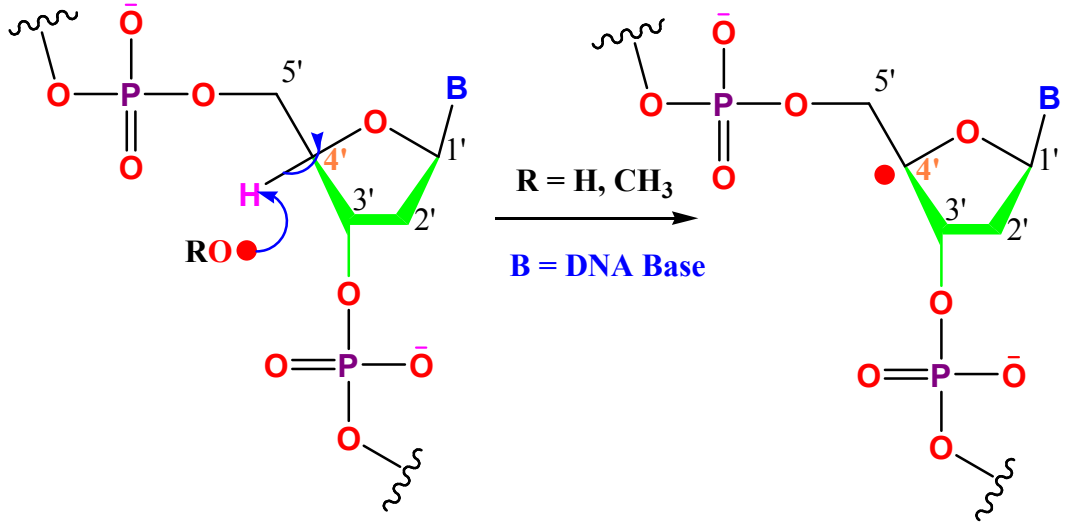

Fig. 11. Hydrogen abstraction from C-4' of DNA sugar

^{1}H NMR spectra of 2-Chloro-3-formyl-quinoline

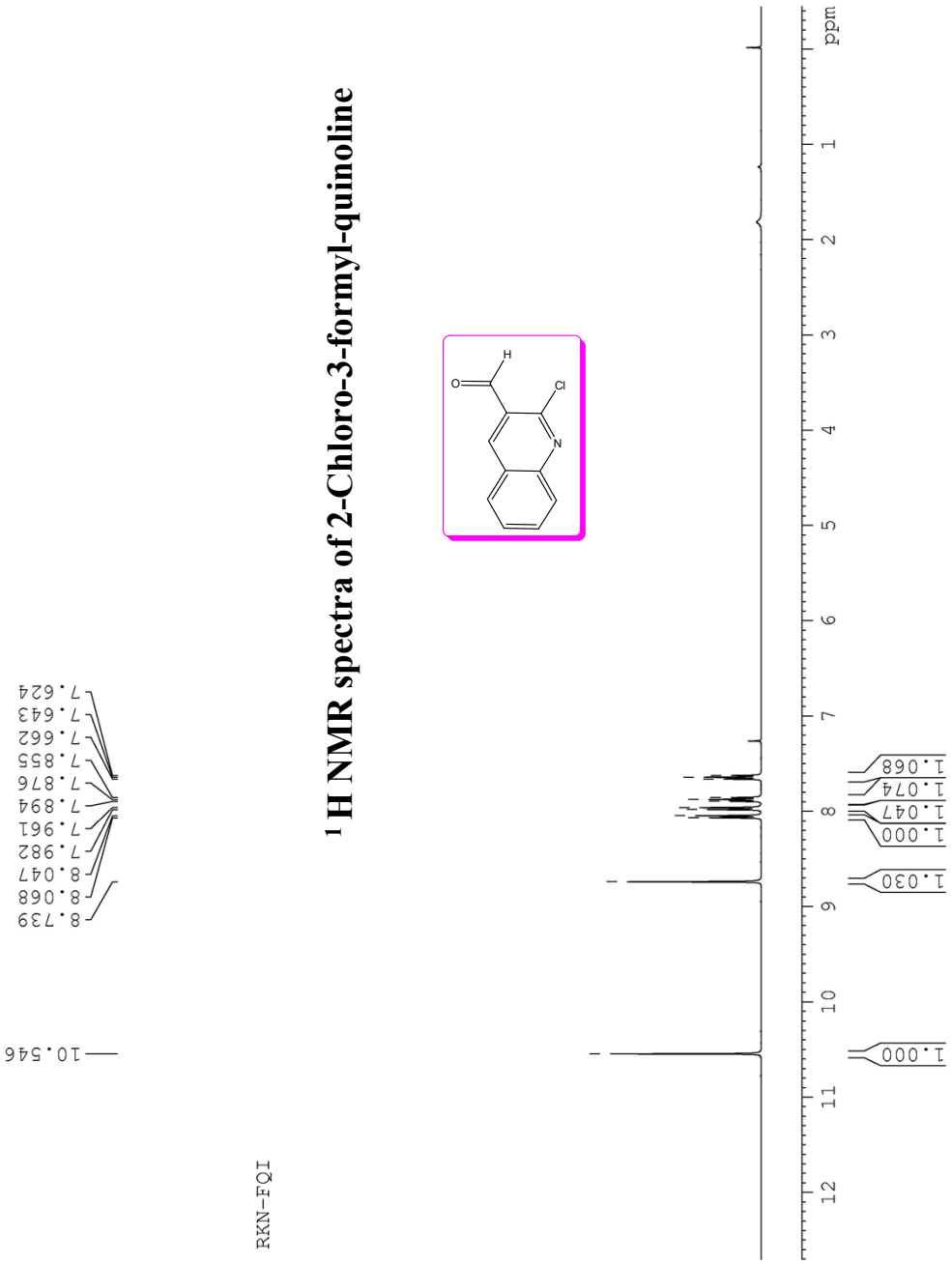

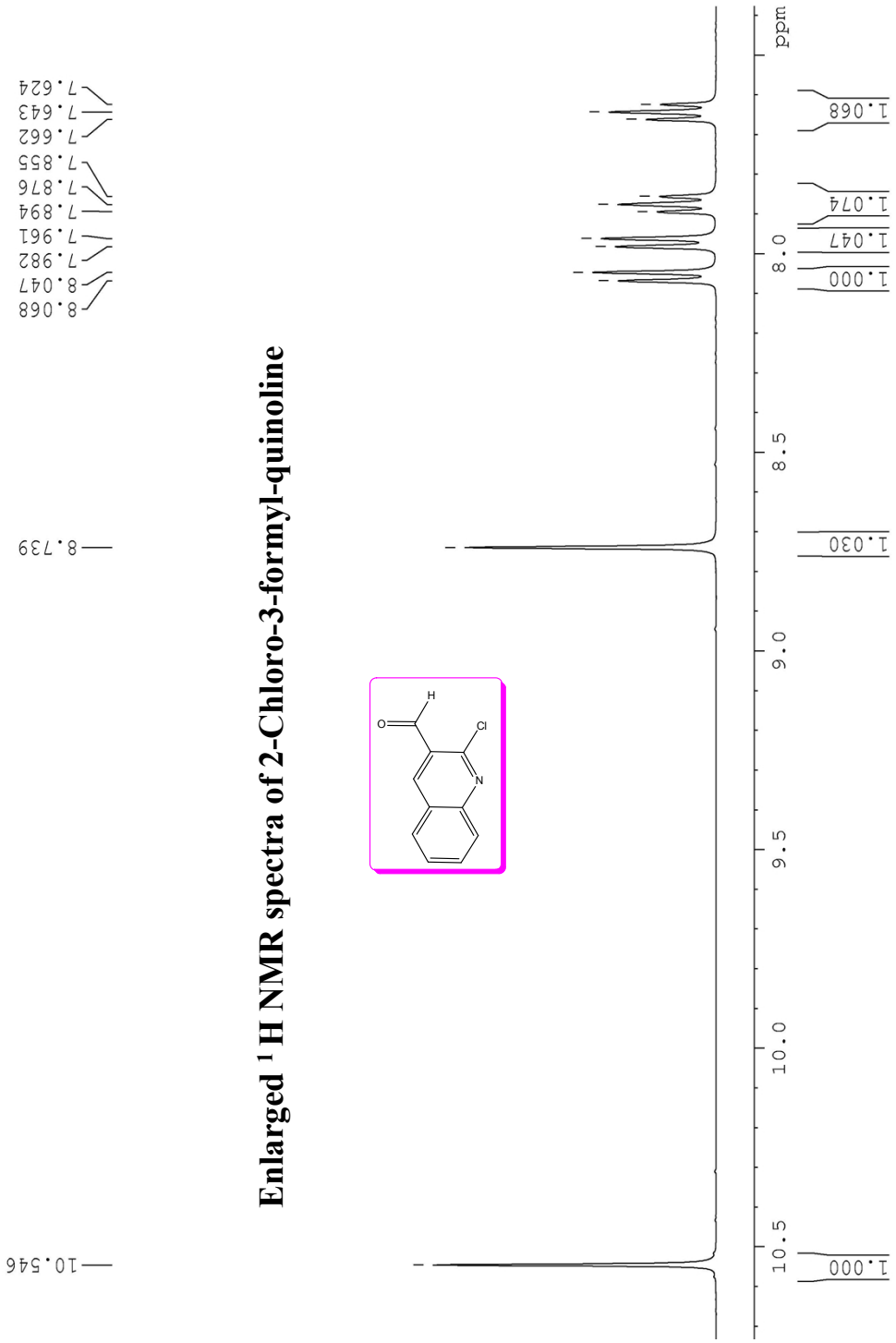
Enlarged ¹H NMR spectra of 2-Chloro-3-formyl-quinoline
ppm
10.5
10.0
9.5
9.0
8.5
8.0
1.000
1.030
1.000
1.047
1.074
1.068
10.546
8.739
8.068
8.047
7.982
7.961
7.894
7.876
7.855
7.662
7.643
7.624
H
O
Cl
N

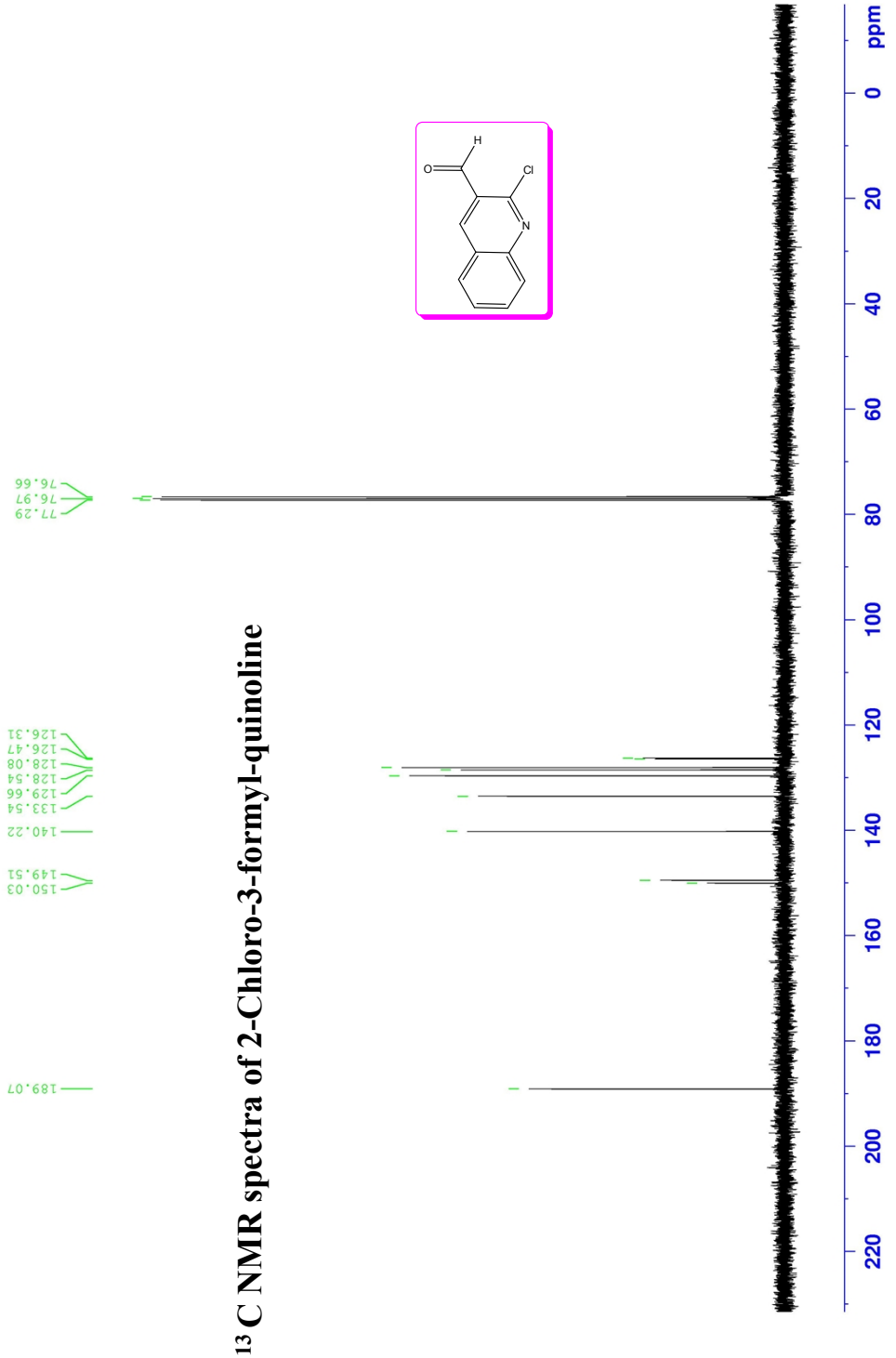
13 C NMR spectra of 2-Chloro-3-formyl-quinoline
H
O
Cl
N
77.29
76.97
76.66
126.31
126.47
128.08
128.54
129.66
133.54
140.22
149.51
150.03
189.07
ppm
0
20
40
60
80
100
120
140
160
180
200
220

^{1}H NMR spectra of 3a

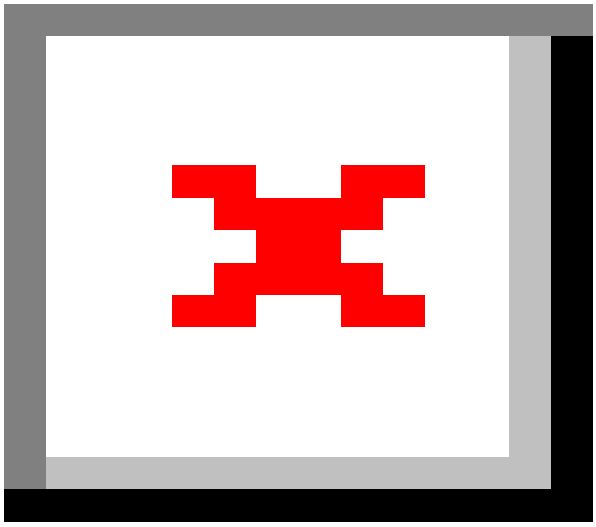

^{1}H NMR spectra of 3b

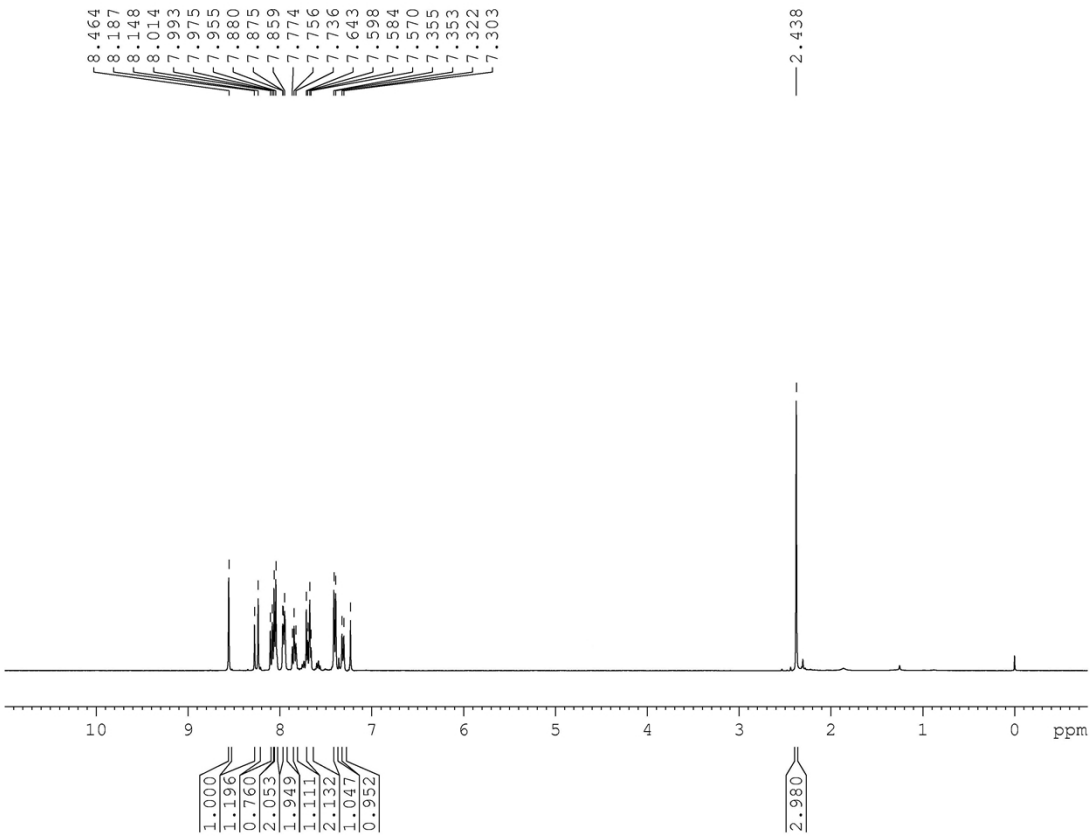

^{13}C NMR spectra of 3b

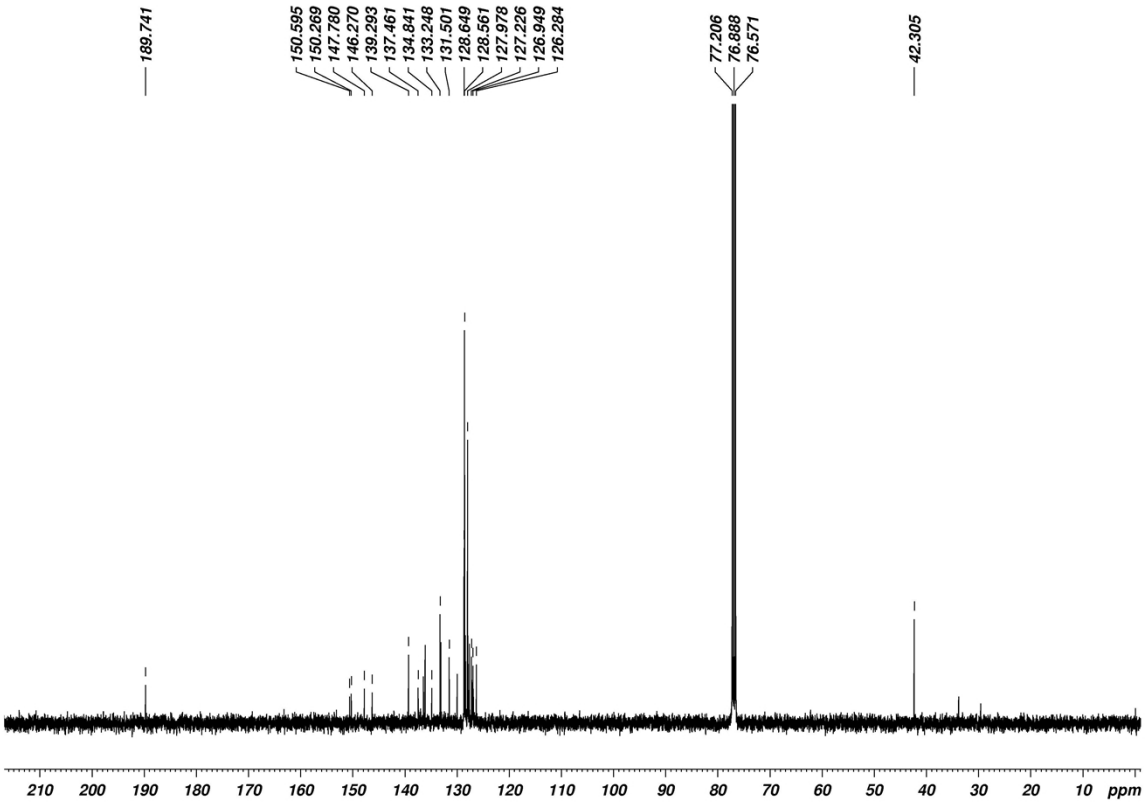

^{1}H NMR spectra of 3c

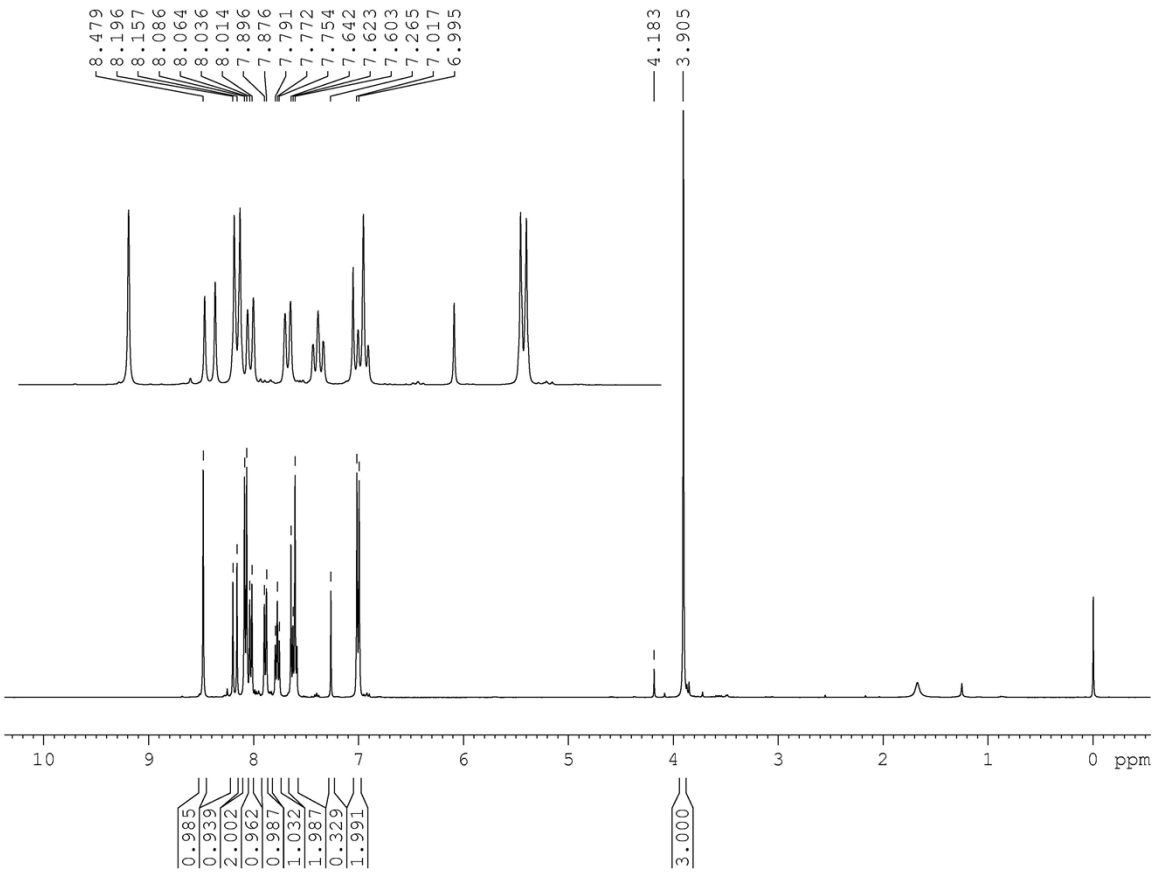

^{13}C NMR spectra of 3c

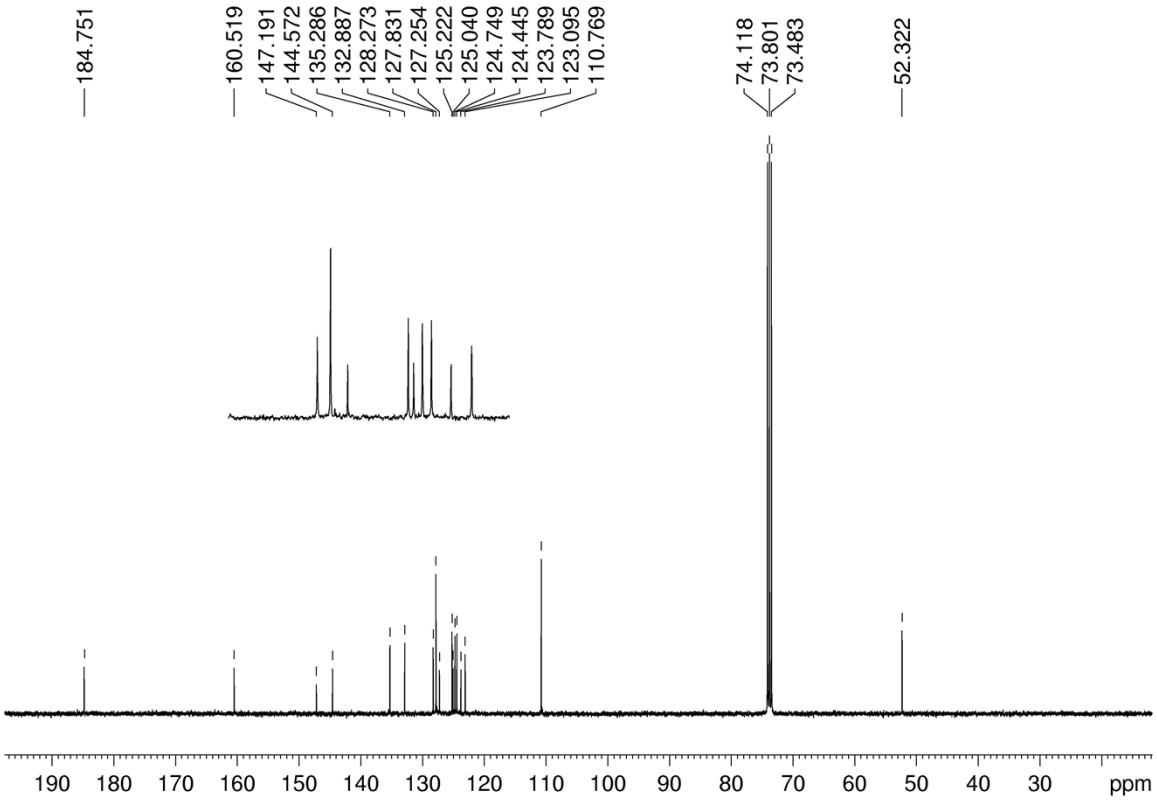

Mass spectra of 3c

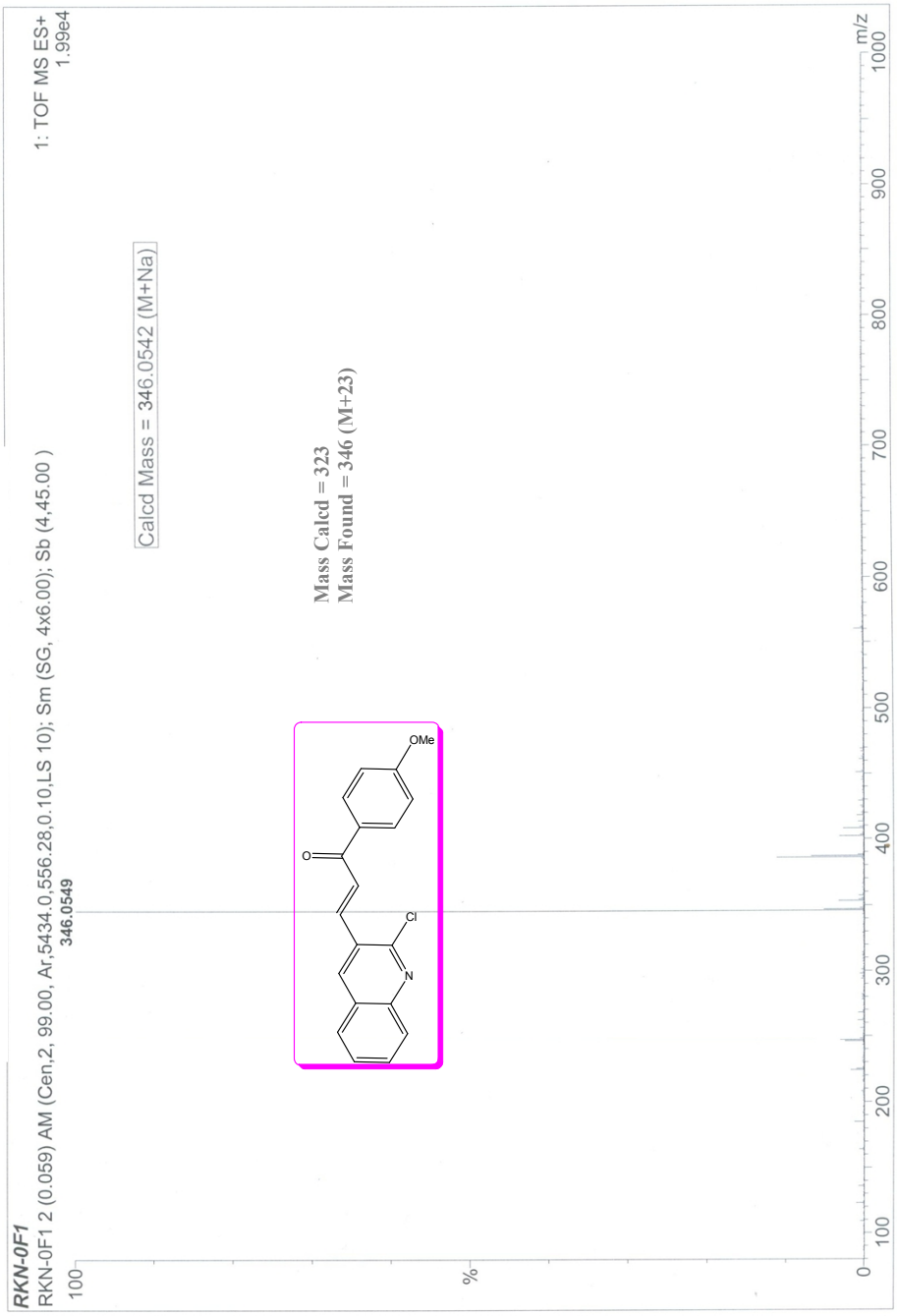

^{1}H NMR spectra of 3d

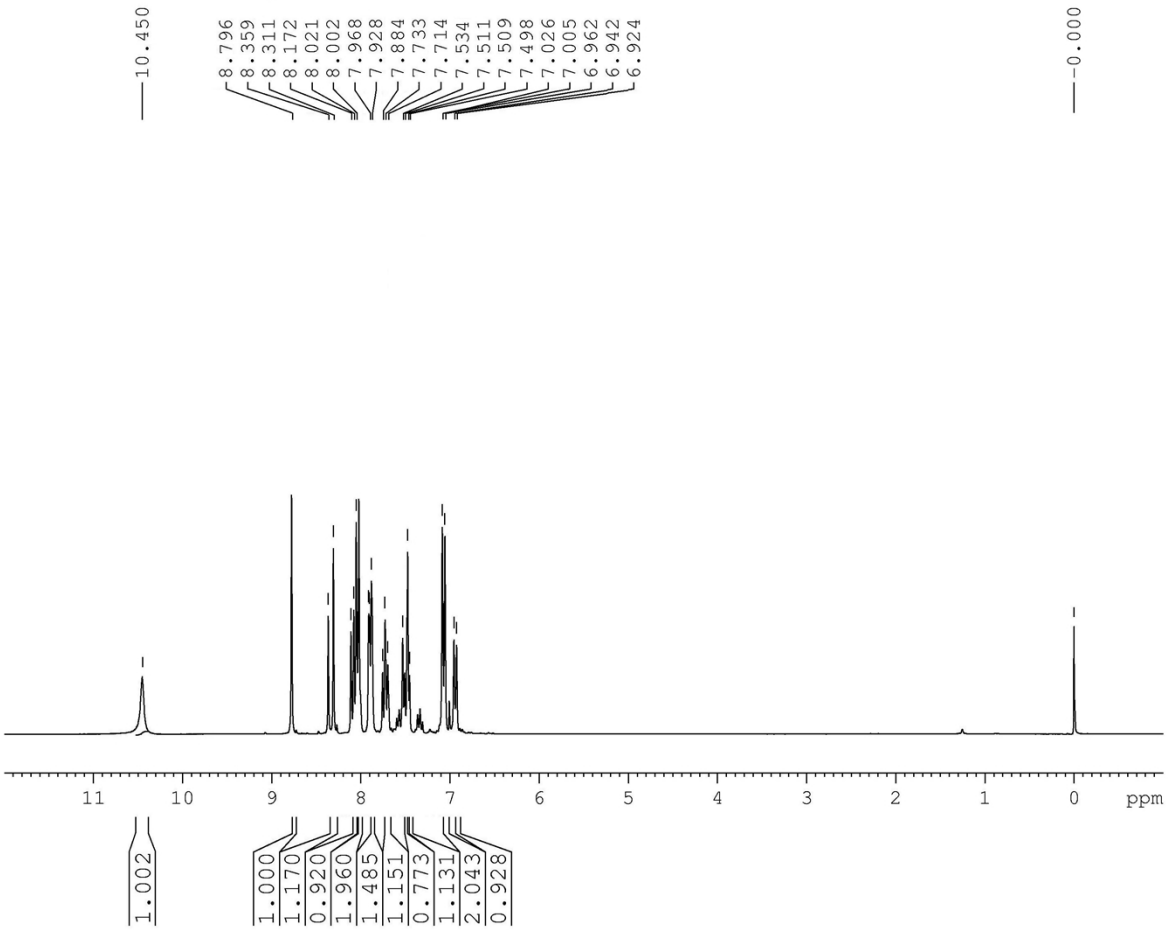

^{13}C NMR spectra of 3d

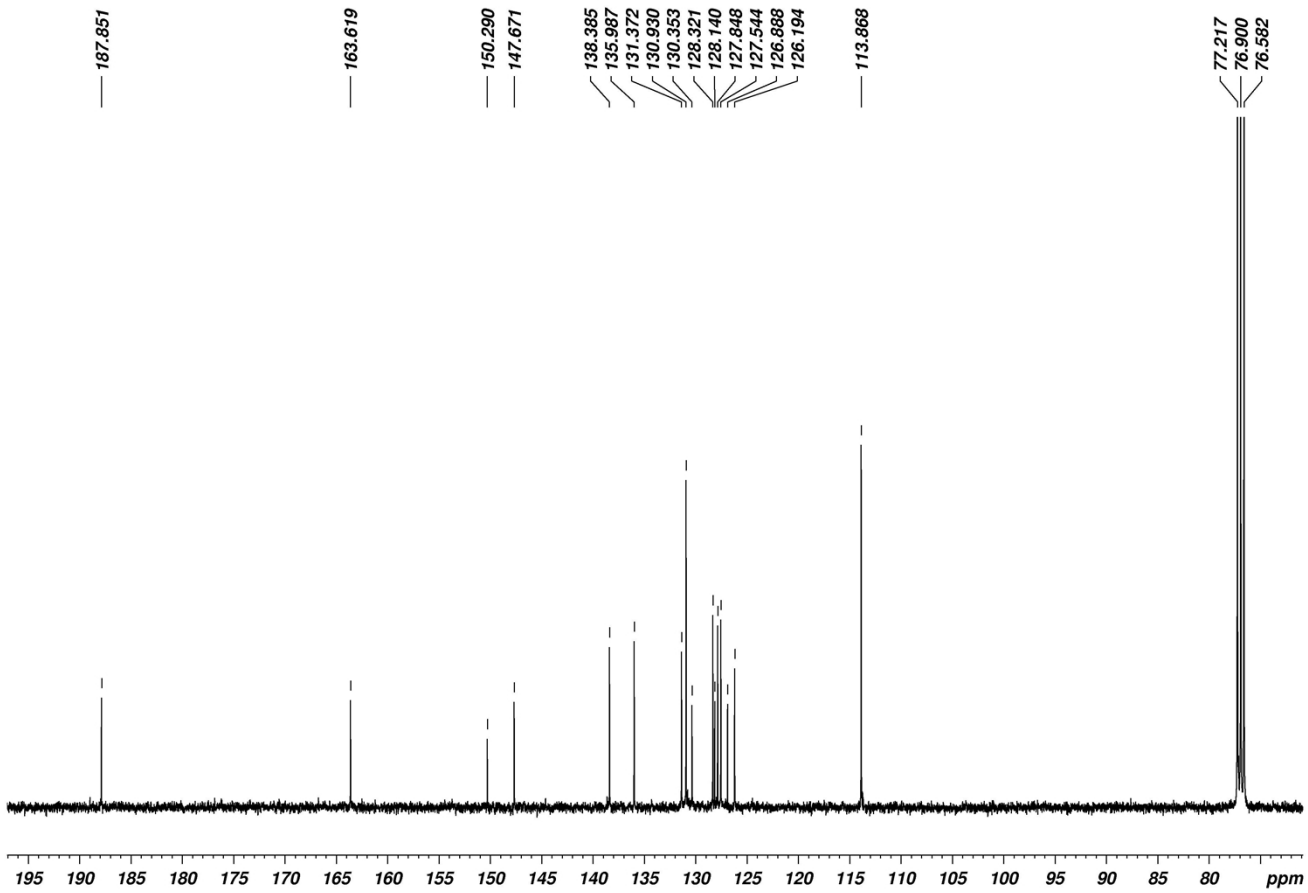

^{1}H NMR spectra of 3e

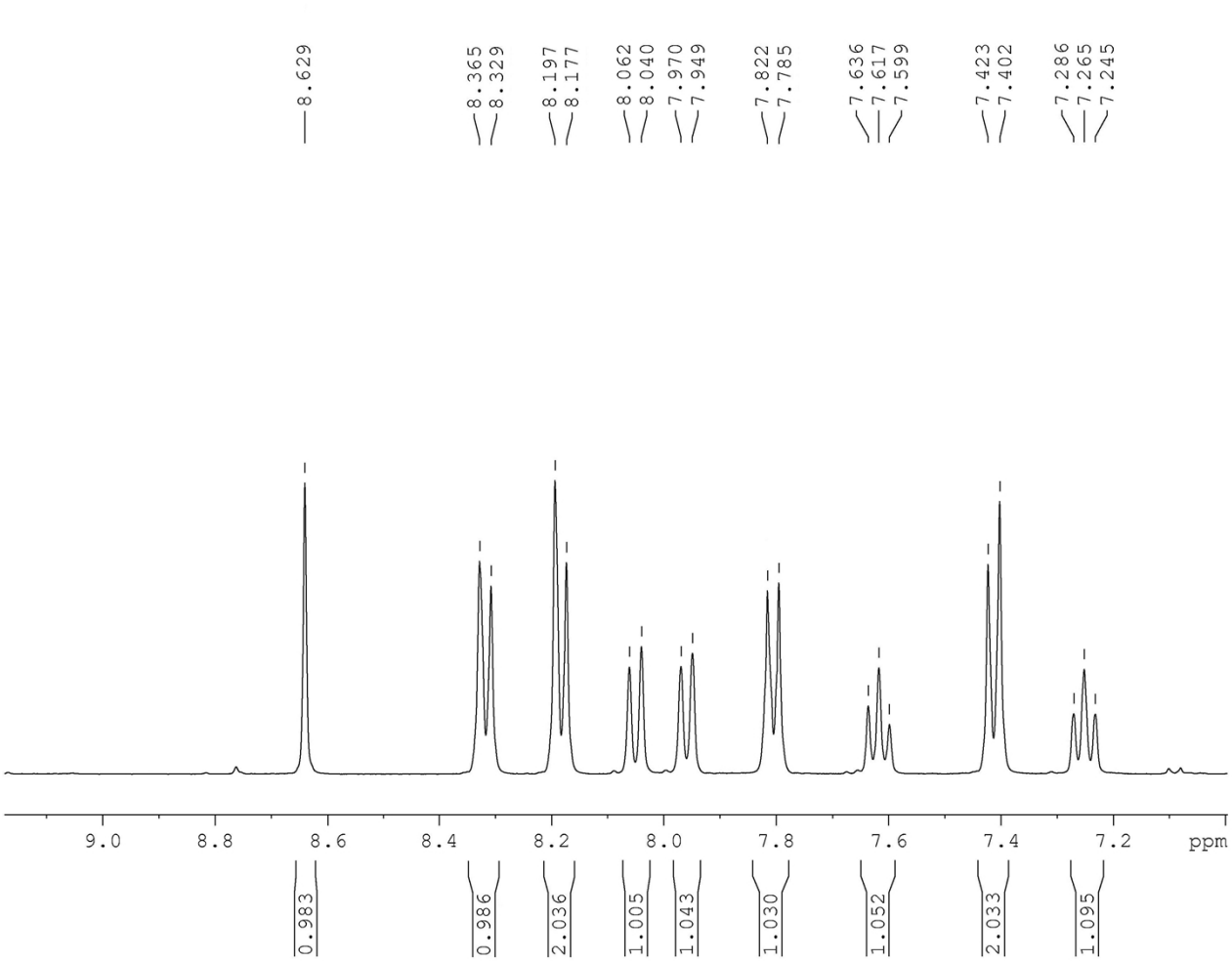

^{13}C NMR spectra of 3e

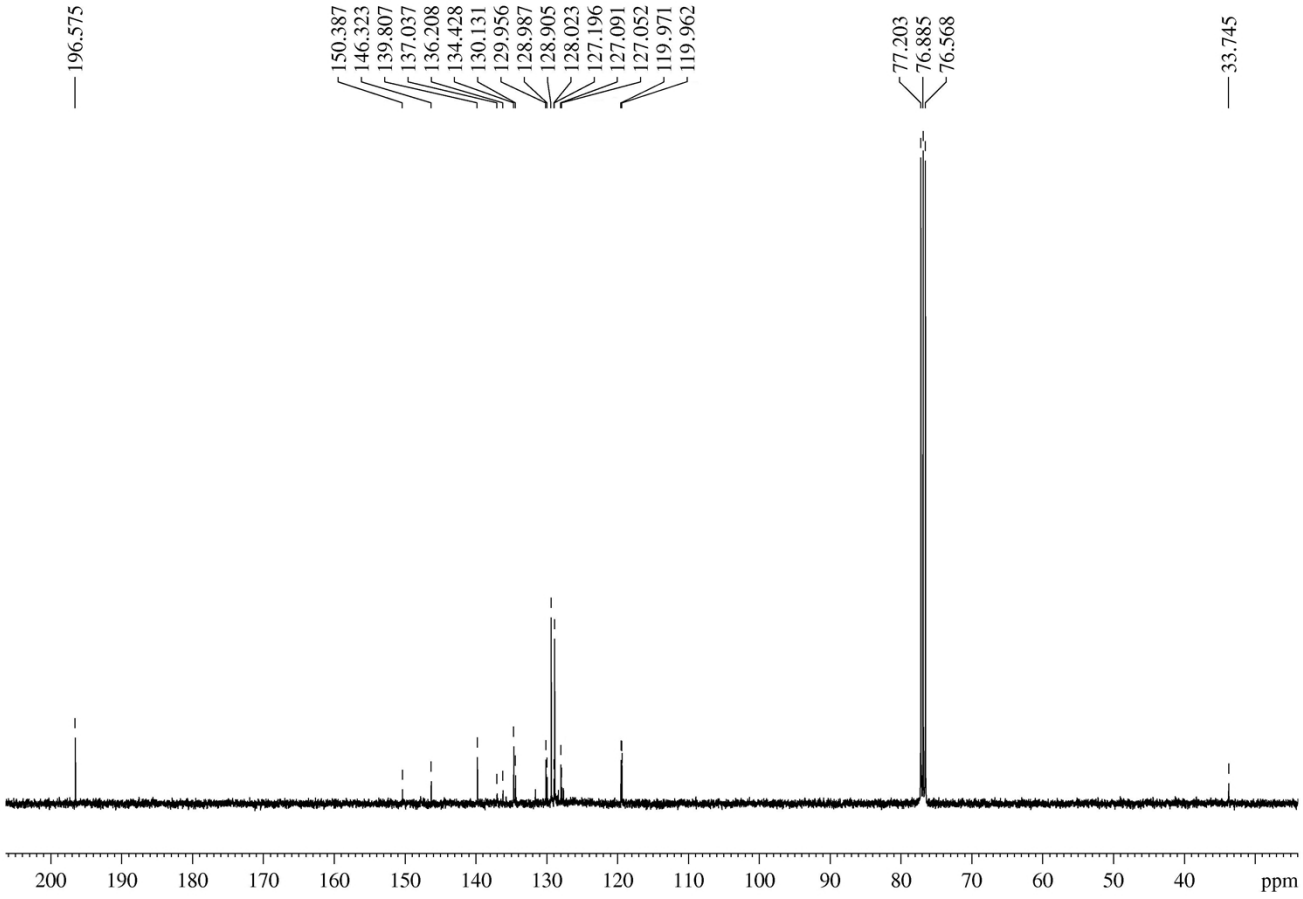

Mass spectra of 3e

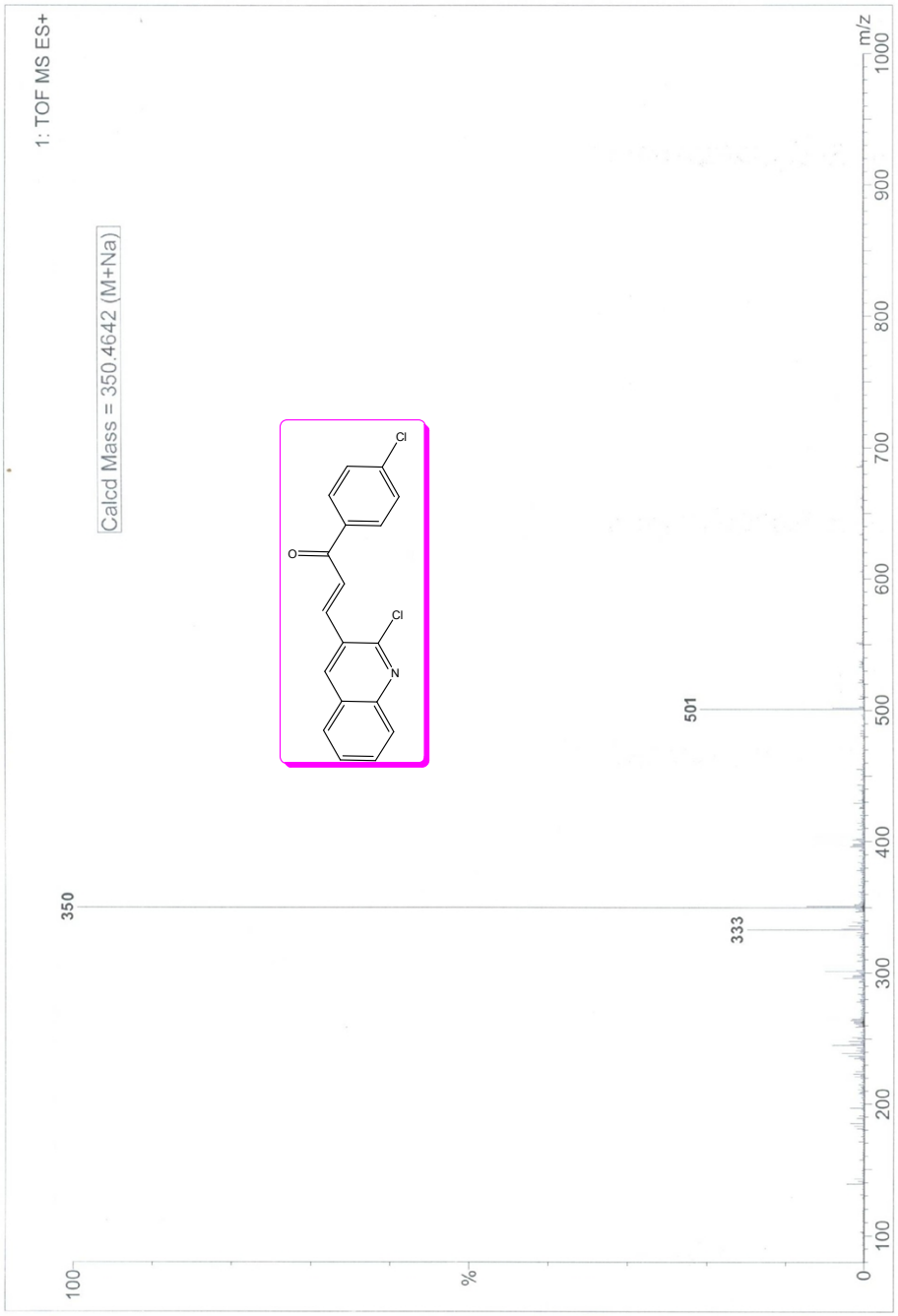

^{1}H NMR spectra of 3h

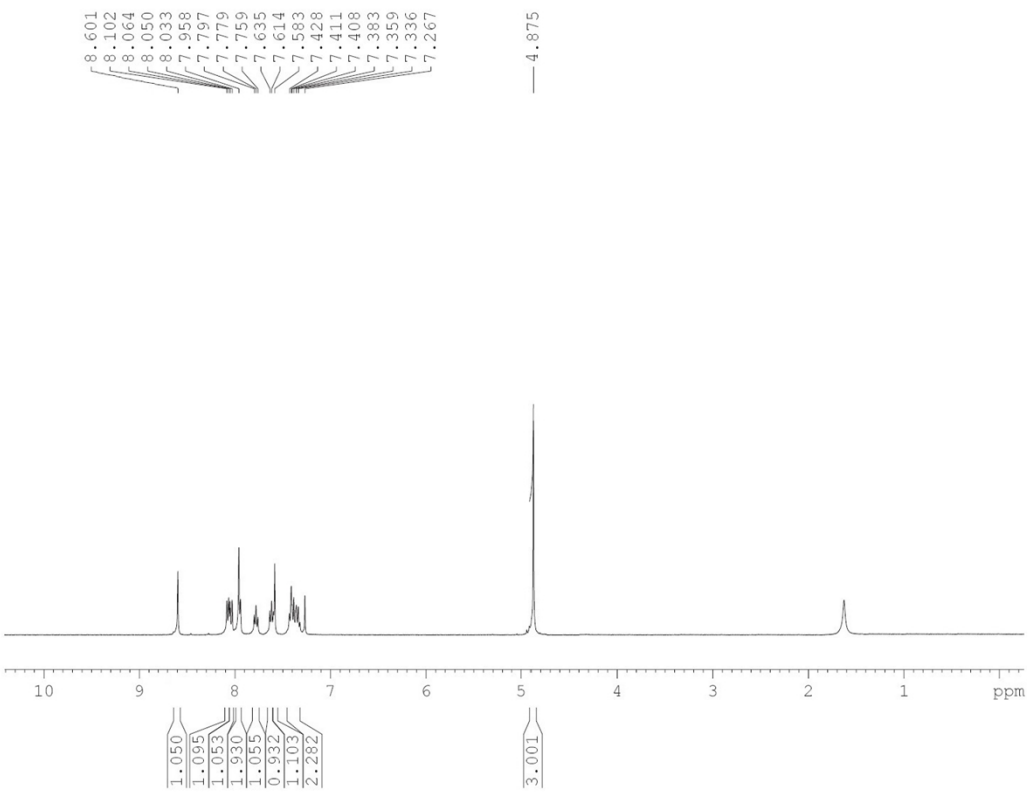

^{13}C NMR spectra of 3h

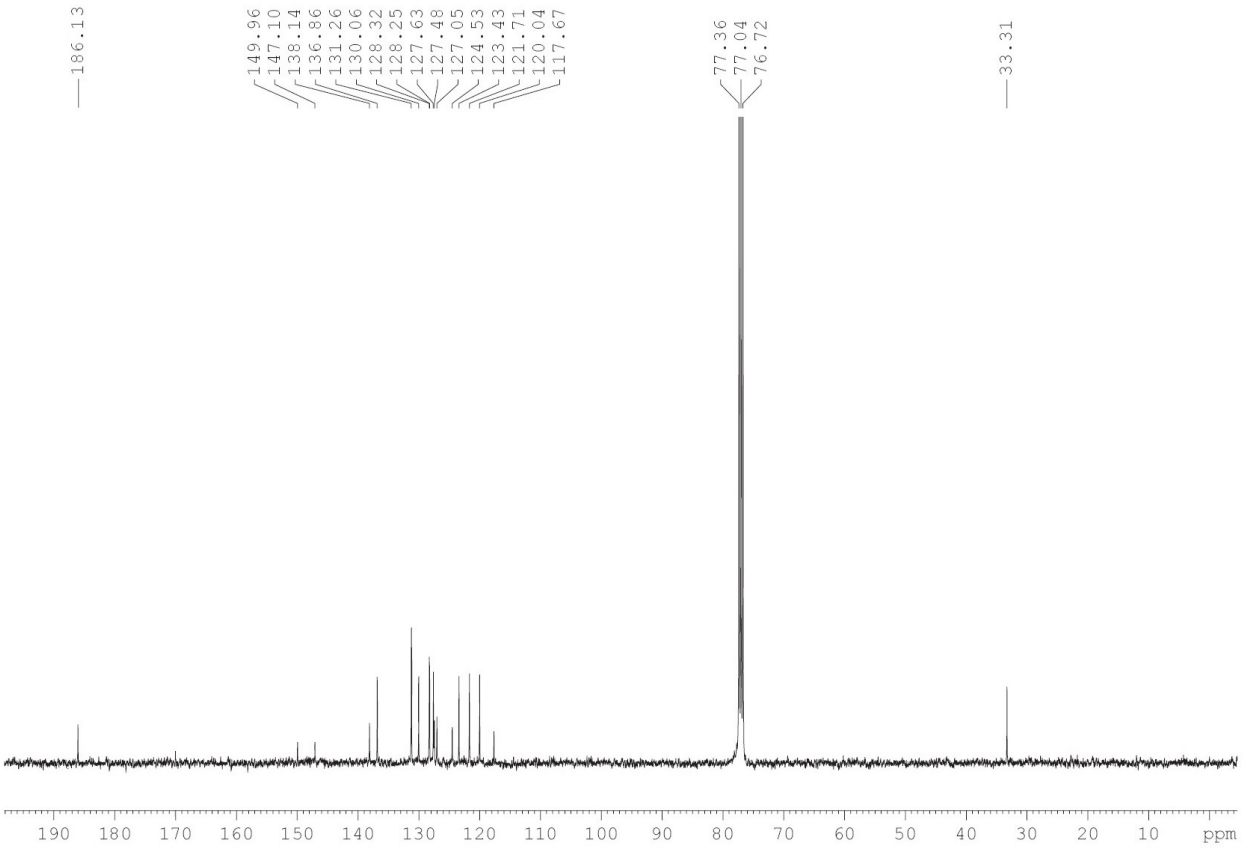

IR spectra of 3a

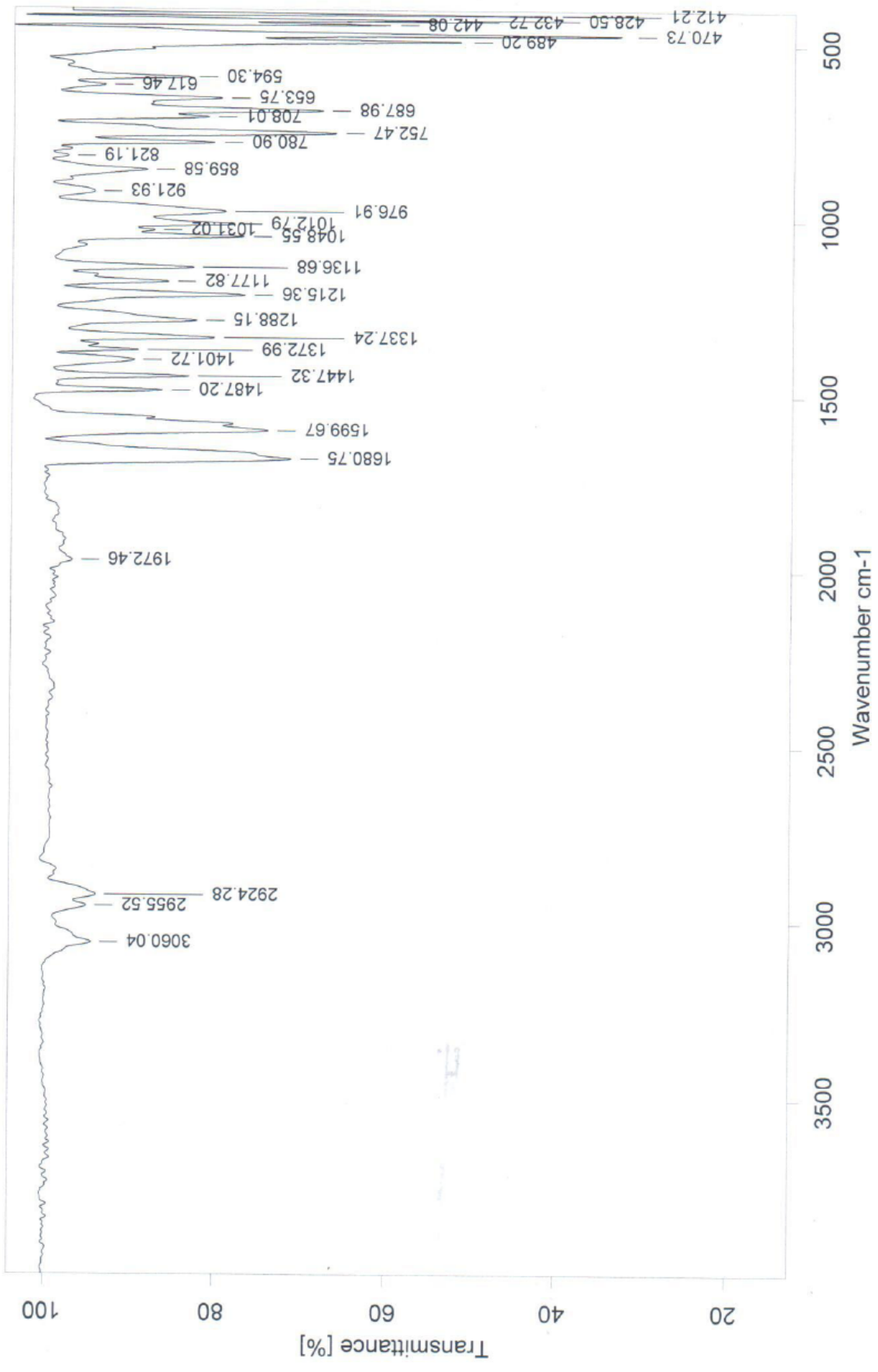

IR spectra of 3b

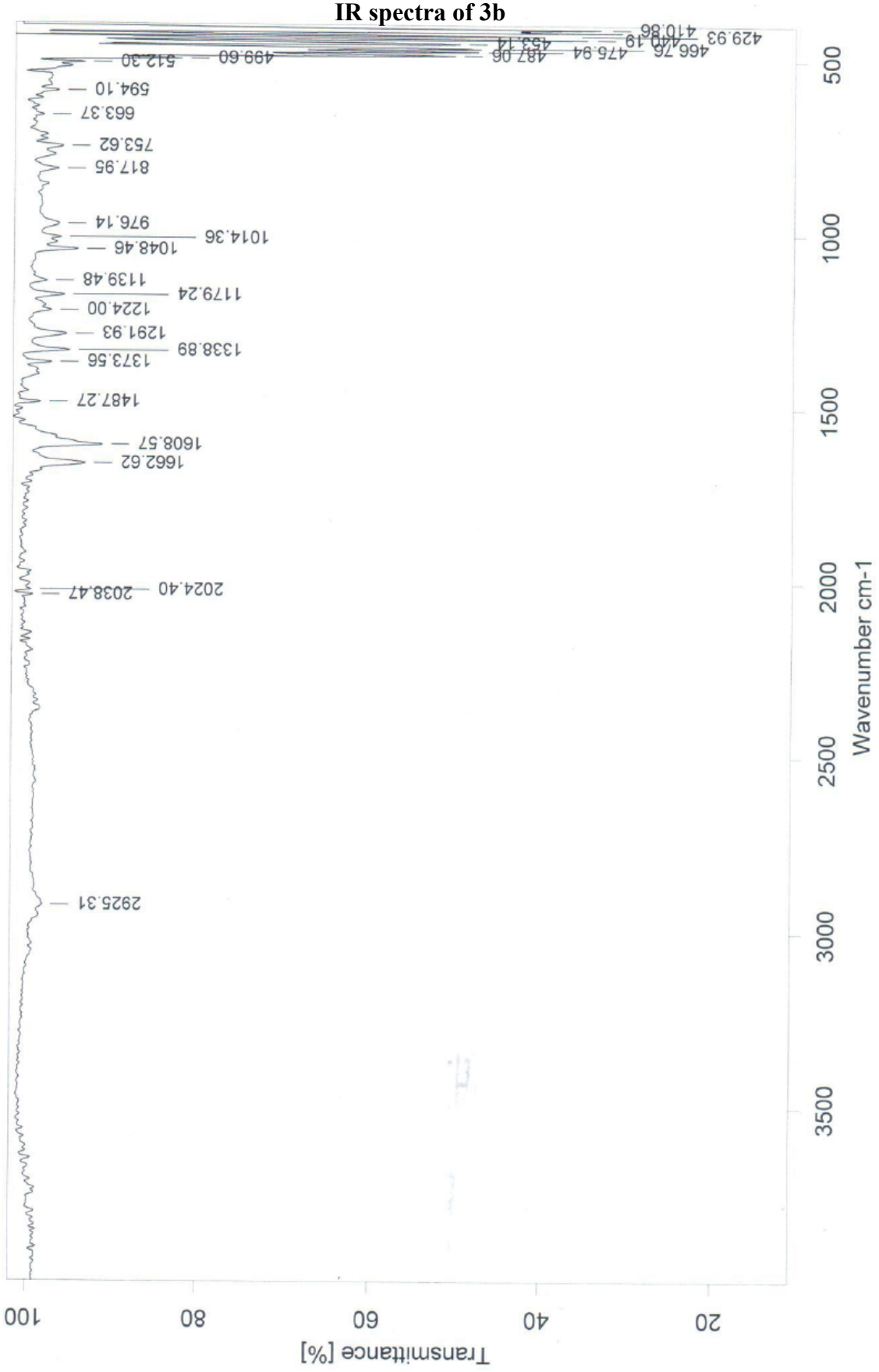

IR spectra of 3c

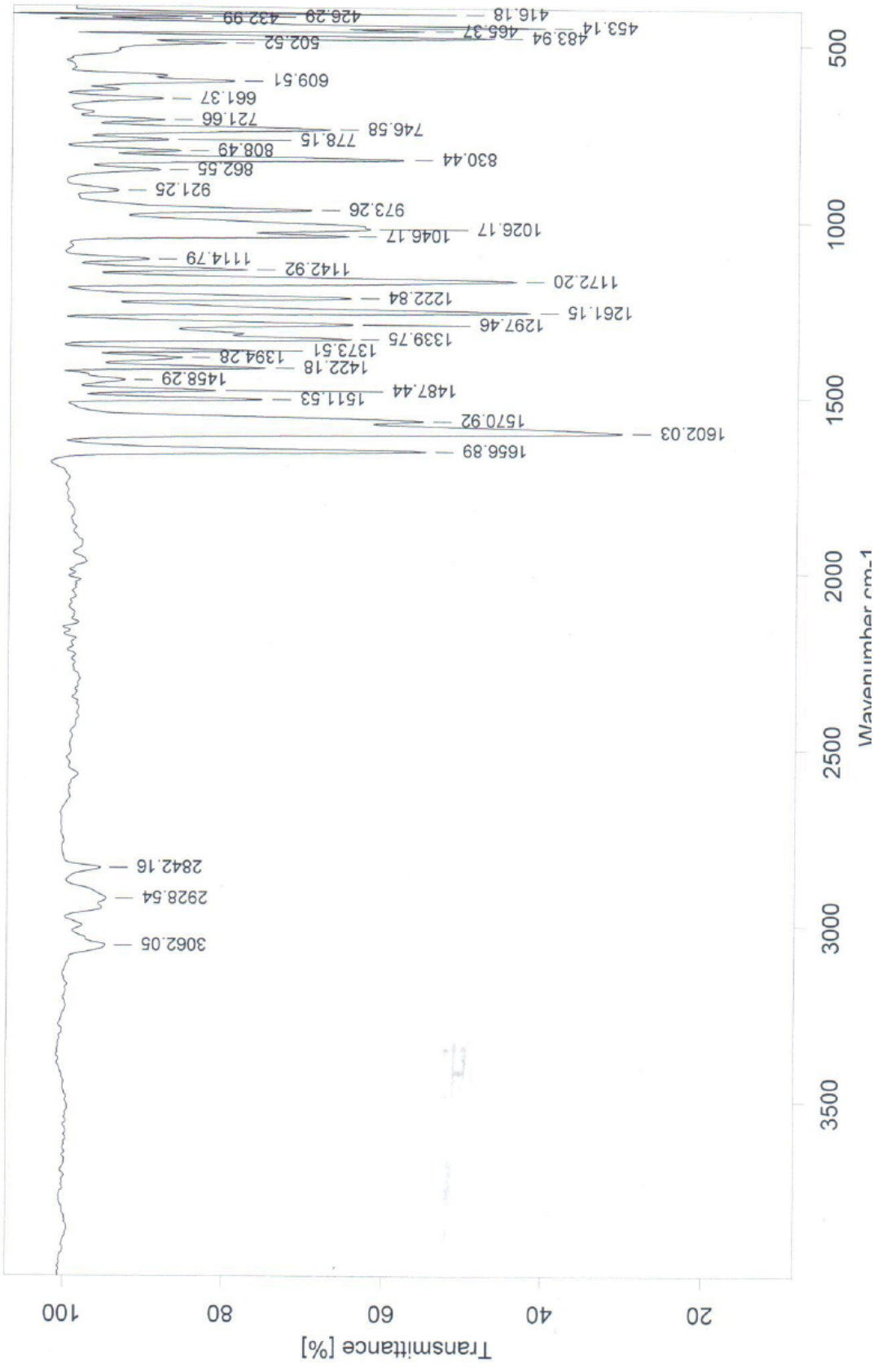

IR spectra of 3d

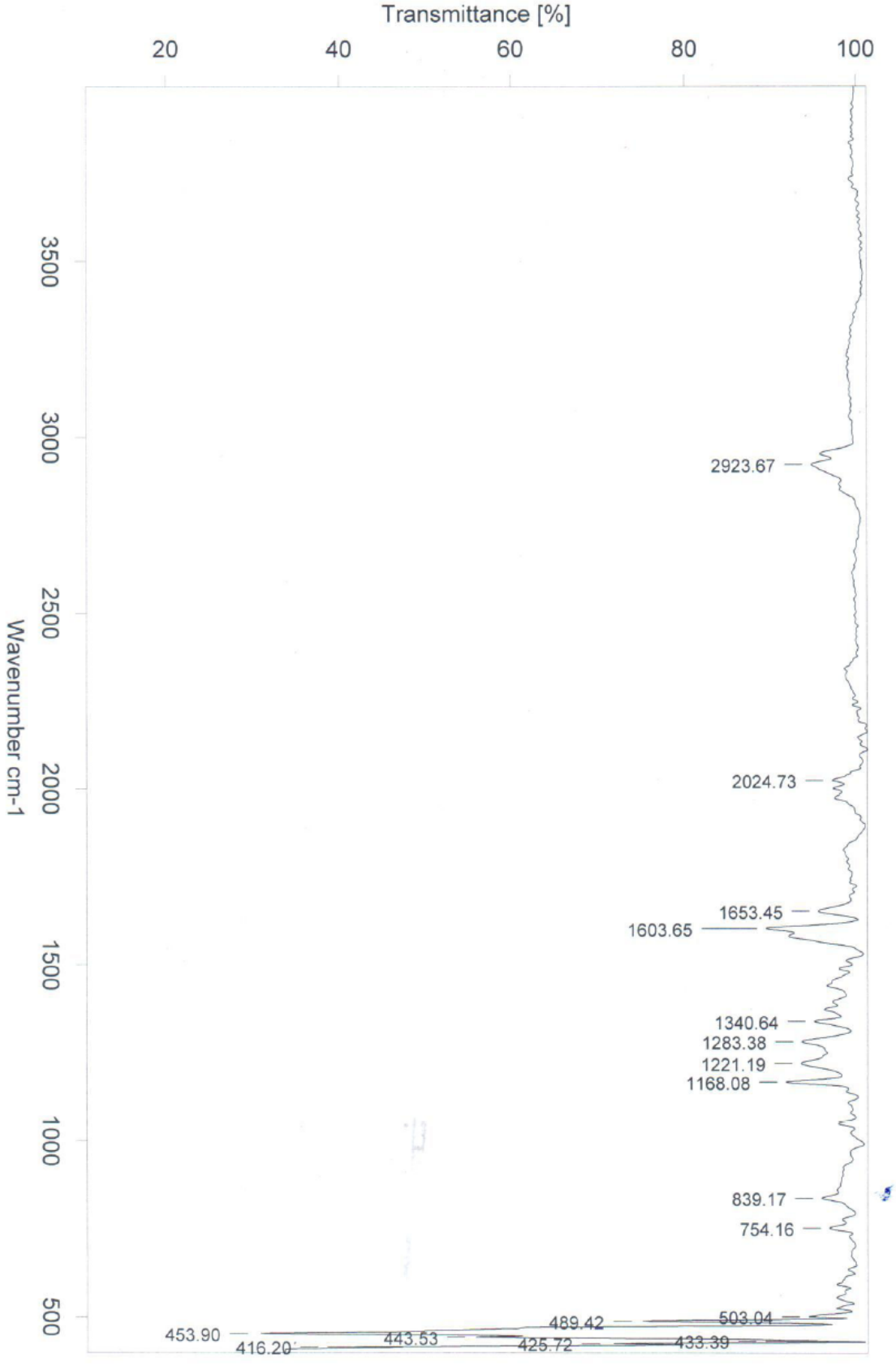

IR spectra of 3e

IR spectra of 3h